Theoretical Astrophysics

Volume I: Astrophysical Processes

T. Padmanabhan

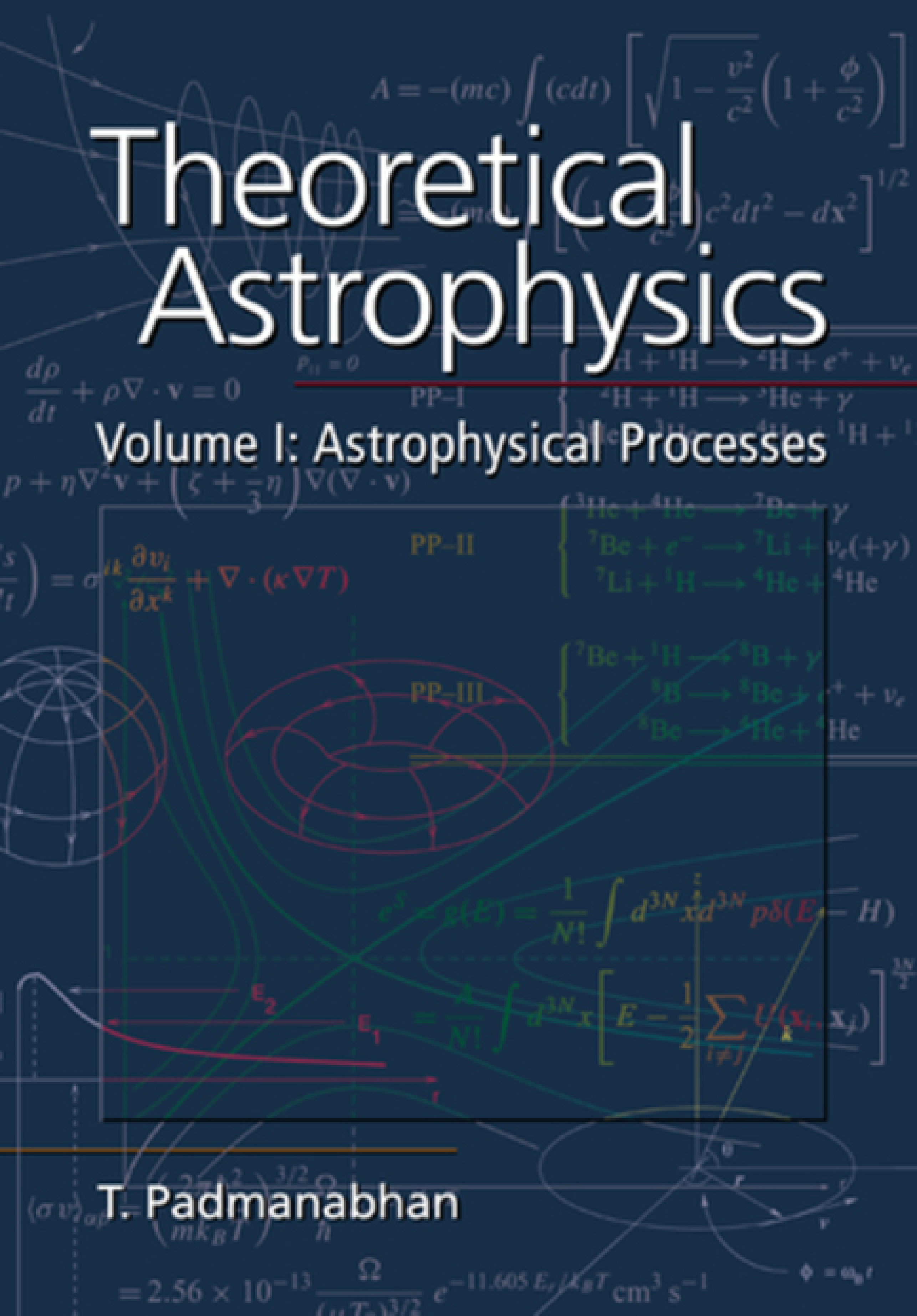

Course of Theoretical Astrophysics

Volume I: Astrophysical Processes

Graduate students and researchers in astrophysics and cosmology need a solid understanding of a wide range of physical processes. This clear and authoritative textbook has been designed to help them to develop the necessary toolkit of theory. Assuming only an undergraduate background in physics and no detailed knowledge of astronomy, this book guides the reader step by step through a comprehensive collection of fundamental theoretical topics. The book is modular in design, allowing the reader to pick and choose a selection of chapters, if necessary. It can be used alone or in conjunction with the forthcoming accompanying two volumes (covering stars and stellar systems and galaxies and cosmology, respectively).

After the basics of dynamics, electromagnetic theory, and statistical physics are reviewed, a solid understanding of all the key concepts such as radiative processes, spectra, fluid mechanics, plasma physics and magnetohydrodynamics, dynamics of gravitating systems, general relativity, and nuclear physics is developed. Each topic is developed methodically from undergraduate basic physics. Throughout, the reader's understanding is developed and tested with carefully structured problems and helpful hints.

This welcome volume provides graduate students with an indispensable introduction to and reference on all the physical processes they will need to tackle successfully cutting-edge research in astrophysics and cosmology.

THANU PADMANABHAN is a Professor at Inter-University Centre for Astronomy and Astrophysics in Pune, India. His research interests are Gravitation, Cosmology, and Quantum Theory. He has published over hundred technical papers in these areas and has written four books: *Structure Formation in the Universe, Cosomology and Astrophysics Through Problems, After the First Three Minutes*, and, together with J.V. Narlikar, *Gravity, Gauge Theories and Quantum Cosmology*.

He is a member of the Indian Academy of Sciences, National Academy of Sciences, and International Astronomical Union. He has received numerous awards, including the Shanti Swarup Bhatnagar Prize in Physics (1996) and the Millenium Medal (2000) awarded by the Council of Scientific and Industrial Research, India.

Professor Padmanabhan has also written more than 100 popular science articles, a comic strip serial, and several regular columns on astronomy, recreational mathematics, and history of science that have appeared in international journals and papers. He is married, has one daughter, and lives in Pune, India. His hobbies include chess, origami, and recreational mathematics.

COURSE OF THEORETICAL ASTROPHYSICS

Volume I: Astrophysical Processes

T. PADMANABHAN

Inter-University Centre for Astronomy and Astrophysics
Pune, India

CAMBRIDGE
UNIVERSITY PRESS

CAMBRIDGE UNIVERSITY PRESS
Cambridge, New York, Melbourne, Madrid, Cape Town, Singapore, São Paulo

Cambridge University Press
The Edinburgh Building, Cambridge CB2 8RU, UK

Published in the United States of America by Cambridge University Press, New York

www.cambridge.org
Information on this title: www.cambridge.org/9780521562409

First published 2000

A catalogue record for this publication is available from the British Library

Library of Congress Cataloguing in Publication data
Padmanabhan, T. (Thanu), 1957–
Theoretical astrophysics : astrophysical processes / T. Padmanabhan.
p. cm.
ISBN 0-521-56240-6
1. Astrophysics. I. Title.
QB461.B33 2000
523.01 – dc21 00-025837

ISBN 978-0-521-56240-9 hardback
ISBN 978-0-521-56632-2 paperback

Transferred to digital printing 2007

Dedicated to the memory of L.D. Landau,
who understood the importance of pedagogy

COURSE OF THEORETICAL ASTROPHYSICS

– in three volumes –

VOLUME I: ASTROPHYSICAL PROCESSES

1: Order-of-magnitude astrophysics; 2: Dynamics; 3: Special Relativity, Electrodynamics, and Optics; 4: Basics of Electromagnetic Radiation; 5: Statistical Mechanics; 6: Radiative Processes; 7: Spectra; 8: Neutral Fluids; 9: Plasma Physics; 10: Gravitational Dynamics; 11: General Theory of Relativity; 12: Basics of Nuclear Physics.

VOLUME II: STARS AND STELLAR SYSTEMS

1: Overview: Stars and Stellar Systems; 2: Stellar Structure; 3: Stellar Evolution; 4: Supernova; 5: White Dwarfs, Neutron Stars, and Black Holes; 6: Pulsars; 7: Binary Stars and Accretion; 8: Sun and Solar System; 9: Interstellar Medium; 10: Globular Clusters.

VOLUME III: GALAXIES AND COSMOLOGY

1: Observational Overview; 2: Galactic Structure; 3: Galactic Dynamics and Interactions; 4: Friedmann Model; 5: Active Galactic Nuclei–Structural Aspects; 6: Thermal History of the Universe; 7: Structure Formation; 8: Cosmic Microwave Background Radiation; 9: Formation of Baryonic Structures; 10: Active Galactic Nuclei–Cosmological Aspects; 11: Intergalactic Medium and Absorption Systems; 12: Cosmological Observations.

Contents

Preface

"...yoyum varo gudham anupravisto,
naanyam thasman Nachiketa vrinithe."
("...Nachiketa does not choose any other boon but
[learning about] that of which Knowledge is hidden.")

Katho Upanishad, Verse 29.

During the past decade or so, theoretical astrophysics has emerged as one of the most active research areas in physics. This advance has also been reflected in the greater interdisciplinary nature of research that is being carried out in this area in the recent years. As a result, those who are learning theoretical astrophysics with the aim of making a research career in this subject need to assimilate considerable amount of concepts and techniques, in different areas of astrophysics, in a short period of time. Every area of theoretical astrophysics, of course, has excellent textbooks that allow the reader to master that *particular* area in a well-defined way. Most of these textbooks, however, are written in a traditional style, focussing on one area of astrophysics (say stellar evolution, galactic dynamics, radiative processes, cosmology etc.) Because different authors have different perspectives regarding their subject matter it is not very easy for a student to understand the key unifying principles behind several different astrophysical phenomena by studying a plethora of separate textbooks, as they do not link up together as a series of core books in theoretical astrophysics covering everything which a student would need. A few books, which *do* cover the whole of astrophysics, deal with the subject at a rather elementary ("first course") level.

What we require is clearly something analogous to the famous Landau–Lifshitz course in theoretical physics, but focussed to the subject of theoretical astrophysics at a fairly advanced level. In such a course, all the key physical concepts (e.g., radiative processes, fluid mechanics, plasma physics, etc.) can be presented from a unified perspective and then applied to different astrophysical situations.

This book is the first of a set of three volumes that are intended to do exactly that. They form one single coherent unit of study through the use of which a student can acquire mastery over all the traditional astrophysical topics. What is more, these volumes emphasise the unity of concepts and techniques in different branches of astrophysics. The interrelationship among different areas and common features in the analysis of different theoretical problems will be stressed throughout. Because many of the basic techniques need to be developed only once, it is possible to achieve a significant economy of presentation and crispness of style in these volumes.

Needless to say, there are some basic "boundary conditions" one has to respect in such an attempt to cover the whole of Theoretical Astrophysics in approximately 3×580 pages. Not much space is available to describe the nuances in greater length or to fill in the details of algebra. For example, I have made conscious choices as to which parts of the algebra can be left to the reader and which need to be worked out explicitly in the text, and I have omitted a detailed discussion of elementary concepts and derivations. However, I do *not* expect the reader to know anything about astrophysics. All astrophysical concepts are developed ab initio in these volumes. The approach used in these three volumes is similar to that used by Gengis Khan, namely, (1) cover as much area as possible, (2) capture the important points, and (3) be utterly ruthless!

To cut out as much repetition as possible, the bulk of the physical principles are presented at one go in Vol. I and are applied in the other two volumes to different situations. This implies that there will be a lot of physics but very little of "concrete" astrophysics in Vol. I; that comes in Vol. II (Stars and Stellar Systems) and Vol. III (Extragalactic Astronomy and Cosmology). The criteria for the selection of material for Vol. I have been the following: (1) Any physical principle that finds application in more than one chapter of Vol. II or Vol. III (for example, bremsstrahlung, Voigt profile, etc.) is discussed in Vol. I. Certain topics that are used in only a specific chapter in Vol. II or Vol. III are discussed in situ rather than in Vol. I. (2) By and large, everything discussed in Vol. I will be utilized directly somewhere in Vols. II and III. On rare occasion, I do cover a topic in Vol. I even if it is not fully utilized in Vol. II or Vol. III because a reader who is going to work in theoretical astrophysics will eventually need an understanding of that particular topic. (3) These three volumes concentrate on *theoretical* aspects. Observation and phenomenology are, of course, discussed in Vols. II and III to the extent necessary to make the motivation clear. However, I do not have the space to discuss how these observations are made, the errors, reliability, etc., of the observations or the astronomical techniques. (Maybe there should be a fourth volume describing observational astrophysics!)

The target audience for this three-volume work will be fairly large and is made up of (1) students in the first year of their Ph.D. Program in theoretical physics, astronomy, astrophysics, and cosmology; (2) research workers in various fields of theoretical astrophysics, cosmology, etc.; and (3) teachers of graduate courses in theoretical astrophysics, cosmology and related subjects. In fact, anyone working in or interested in some area of astronomy or astrophysics will find something useful in these volumes. They are also designed in such a way that parts of the material can be used in modular form to suit the requirements of different people and different courses.

Let me briefly highlight the features which are specific to Vol. I. The reader of Vol. I is assumed to have done basic courses in classical mechanics, nonrelativistic quantum mechanics, and classical electromagnetic theory. Of the 12 chapters in Vol. I, the first one is a broad-brush overview of physical principles in an order-of-magnitude manner and is intended to set the stage. I expect the reader to survey this chapter rapidly but to come back to it periodically at later stages. This chapter is probably the easiest or the most difficult, depending on one's background and aptitude. It is easy in the sense that very little sophisticated mathematics is used; difficult because it takes a high level of maturity to appreciate some of the physical arguments that are presented. Chapters 2 (Dynamics), 3 (Special Relativity, Electrodynamics, and Optics), and 5 (Statistical Mechanics) cover the ground the reader may already be familiar with – but from an advanced perspective. The aim is to introduce powerful techniques in familiar contexts so that the reader can learn and appreciate them. For example, no apologies are made for introducing four-vector notation up front or dealing with distribution functions right from the beginning, so as to get the main results as quickly as possible. The emphasis throughout is on topics relevant in astrophysics, such as the reduced three-body problem, action-angle variables, diffraction and interference, optical systems, propagation in random media, ionisation equilibria, etc. Chapter 4 deals with the basics of radiation theory – both classical and quantum – that is developed from scratch and the reader is *not* assumed to be familiar with quantum field theory.

Chapters 6–12 develop the toolkit for astrophysics in a self-contained manner, virtually ab initio. Chapters 6 (Radiative Processes) and 8 (Fluid Mechanics) are fairly exhaustive and detailed. The short chapter on Spectra (Chap. 7) covers general material that is of astronomical relevance; more specific aspects will be dealt with in Vols. II and III within the appropriate contexts. In Chap. 9 (Plasma Physics) I had to make choices as to which topics are of sufficiently general nature to appear in Vol. I; some specific topics (e.g., instability of axisymmetric systems with magnetic fields, alpha effect, and dynamos) will appear in the relevant chapters of Vols. II and III. Chapter 10 (Gravitational Dynamics) covers the background needed for galactic dynamics, globular cluster evolution, etc. Chapter 11 is a compact introduction to general relativity and *no* previous familiarity with tensor analysis is assumed. Finally, Chap. 12 deals with aspects of nuclear physics that are needed in the study of stellar evolution.

Any one of these topics is fairly vast and often requires a full textbook to do justice to it, whereas I have devoted approximately 60 pages to each of them!

I would like to emphasise that such a crisp, condensed discussion is not only possible but also constitutes a basic matter of policy in these volumes. After all, the idea is to provide the student with the essence of several textbooks in one place. It should be clear to lecturers that these material can be easily regrouped to serve different graduate courses at different levels, especially when complemented by other textbooks.

Because of the highly pedagogical nature of the material covered in Vol. I, I have not given detailed references to original literature except on rare occasions when a particular derivation is not available in standard textbooks. The annotated list of references given at the end of the book cites several other textbooks that I found very useful. Some of these books, of course, contain extensive bibliographies and references to original literature. The selection of core books cited here clearly reflects the personal bias of the author and I apologise to anyone who feels that their work or contribution has been overlooked.

Several people have contributed to the making of these volumes and especially to Vol. I. The idea for these volumes originated over a dinner with J.P. Ostriker in late 1994, while I was visiting Princeton. I was lamenting to Jerry about the lack of a comprehensive set of books covering all of theoretical astrophysics and Jerry said, "Why don't *you* write them?" He was very enthusiastic and supportive of the idea and gave extensive comments and suggestions on the original outline I produced in the next one week. I am grateful to him for the comments and for the moral support that I needed to launch into such a project. I sincerely hope the volumes do not disappoint him.

Adam Black of Cambridge University Press took up the proposal with his characteristic enthusiasm and initiative; this is the third project on which we worked together and I thoroughly enjoyed it. I should also thank him for choosing six excellent (anonymous) referees for this proposal whose support and comments helped to mould the proper framework.

Many of my friends and colleagues carried out the job of reading the earlier drafts and providing comments. Of these, M. Vivekanand has gone through most of the book with meticulous care and has given extensive comments. Many other colleagues, especially Roger Blandford, George Djorgovsky, Peter Goldreich, John Huchra, Donald Lynden-Bell, J.V. Narlikar, R. Nityananda, Sterl Phinney, and Douglas Richstone looked at the whole draft and provided comments and suggestions at different levels of detail. J.S. Bagla, Sai Iyer, Nissim Kanekar, Ben Oppenheimer, K. Subramanian, S. Sankaranarayanan, and K. Srinivasan gave detailed comments on selected chapters; the last two took pains to check most of the derivations and algebraic expressions. I thank all of them for their help.

I have been visiting the Astronomy Department of Caltech during the past several years and the work on this book has benefitted tremendously through my discussions and interactions with the students and staff of the Caltech Astronomy Department. I especially thank Roger Blandford, Peter Goldreich, Shri Kulkarni, Sterl Phinney, and Tony Readhead for several useful discussions and for sharing with me their insights and experience in physics teaching.

This project would not have been possible but for the dedicated support from Vasanthi Padmanabhan, who not only did the entire TEXing and formatting but also produced most of the figures – often writing the necessary programs for the same. I thank her for the help and look forward to receiving the same for the next two volumes! I also thank Sunu Engineer who was resourceful in solving several computer-related problems that cropped up periodically. It is a pleasure to acknowledge the library and other research facilities available at the Inter-University Centre for Astronomy and Astrophysics, which were useful in this task.

T. Padmanabhan

1
Order-of-Magnitude Astrophysics

1.1 Introduction

The subject of astrophysics involves the application of the laws of physics to large macroscopic systems in order to understand their behaviour and predict new phenomena. This approach is similar in spirit to the application of the laws of physics in the study of, say, condensed-matter phenomena, except for the following three significant differences:

(1) We have far less control over the external conditions and parameters in astrophysics than in, say, condensed-matter physics. It is not possible to study systems under controlled conditions so that certain physical processes dominate the behaviour. Identifying the causes of various observed phenomena in astrophysics will require far greater reliance on statistical arguments than in laboratory physics.

(2) The astrophysical systems of interest span a wide range of parameter space and require inputs from several different branches of physics. Typically, the densities can vary from 10^{-25} gm cm^{-3} (interstellar medium) to 10^{15} gm cm^{-3} (neutron stars); temperatures from 2.7 K (microwave background radiation) to 10^9 K (accreting x-ray sources) or even to 10^{15} K (early universe); radiation from wavelengths of meters (radio waves) to fractions of angstroms (hard gamma rays); typical speeds of particles can go up to $0.99c$ (relativistic jets). Clearly we require inputs from quantum-mechanical and relativistic regimes as well as from more familiar classical physics.

(3) The primary source of information about distant astrophysical sources is the electromagnetic radiation detected from them. Therefore, to obtain a complete picture about any source, it is necessary to examine it in all the wave bands. Because of technological limitations, it is often quite difficult to have uniform coverage across the entire electromagnetic spectrum. Hence the information we have about the sources is often distorted or incomplete.

These considerations suggest that two aspects will be most important in the study of different astrophysical systems. The first is the appreciation of the different states in which bulk matter can exist under different conditions and the dynamics of the matter governed by different equations of state. The second is an understanding of different radiative processes that lead to the emission of photons, which act as prime carriers of information about astronomical objects.

We shall be concerned with these and related topics in several chapters of this book. The purpose of this introductory chapter is twofold: It will first provide – in Sections (1.2) – (1.4) – a rapid overview of several physical processes at an order-of-magnitude level and introduce the necessary concepts. Then we will make an attempt to understand the existence of different astrophysical structures from first principles to the extent possible. Implementing such a plan, of course, has not been possible even in laboratory physics, and it is unlikely to succeed in the case of astrophysics. At present, astrophysics does require a fair amount of observational and phenomenological input, just like any other branch of applied physics. Nevertheless, we will make such an attempt as it is useful in providing the most basic and direct connection between physics and astrophysics.

1.2 Energy Scales of Physical Phenomena

Let us consider a system of N particles ($N \gg 1$), each of mass m, occupying a spherical region of radius R. In dealing with the dynamics of such a large collection of particles, it is useful to introduce the concept of pressure exerted by the system of particles as the momentum transferred per second normal to a (fictitious) surface of unit area. The contribution to the rate of momentum transfer (per unit area) from particles of energy ϵ is $n(\epsilon)\mathbf{p}(\epsilon) \cdot \mathbf{v}(\epsilon)$, where $n(\epsilon)$ denotes the number of particles per unit volume with momentum $\mathbf{p}(\epsilon)$ and velocity $\mathbf{v}(\epsilon)$. We obtain the net pressure by averaging this expression over the angles defined by $\mathbf{p}$ (or $\mathbf{v}$) and summing over all values of the energy. Because the momentum and the velocity are parallel to each other, the vector dot product $\mathbf{p} \cdot \mathbf{v}$ averages to $(1/3)pv$ (in three dimensions), giving

$$P = \frac{1}{3} \int_0^\infty n(\epsilon) p(\epsilon) v(\epsilon) \, d\epsilon, \tag{1.1}$$

where the integration is over all energies. The system is called ideal if the kinetic energy dominates over the interaction energy of the particles. In that case ϵ is essentially the kinetic energy of the particle. With the relations

$$p = \gamma m v, \quad \epsilon = (\gamma - 1) m c^2, \quad \gamma \equiv \left(1 - \frac{v^2}{c^2}\right)^{-1/2}, \tag{1.2}$$

where ϵ is the kinetic energy of the particle, the pressure can be expressed in the form

$$P = \frac{1}{3}\int_0^\infty n\epsilon\left(1 + \frac{2mc^2}{\epsilon}\right)\left(1 + \frac{mc^2}{\epsilon}\right)^{-1} d\epsilon. \tag{1.3}$$

In the nonrelativistic (NR) limit (with $mc^2 \gg \epsilon$), this gives $P_{\rm NR} \approx (2/3)\langle n\epsilon\rangle = (2/3)U_{\rm NR}$, where $U_{\rm NR}$ is the energy density (i.e., energy per unit volume) of the particles. In the relativistic case (with $\epsilon \gg mc^2$ or when the particles are massless), the corresponding expression is $P_{\rm ER} \approx (1/3)\langle n\epsilon\rangle = (1/3)U_{\rm NR}$. Hence, in general, $P \approx U$ up to a factor of order unity.

This result can be converted into a more useful form of equation of state whenever the mean free path of the particles in the system is small compared with the length scales over which the physical parameters of the system change significantly. Then the pressure can be expressed in terms of density and temperature if the energy density can be expressed in terms of these variables. This is possible in several contexts leading to different equations of state. To understand each of these cases it is useful to start by identifying the characteristic energy scales of bulk matter. We now turn to this task.

1.2.1 Rest-Mass Energy

We can associate the rest-mass energy mc^2 with each individual particle of mass m. In normal matter, made up of nucleons and electrons, the lowest value for rest-mass is provided by electrons with $m_ec^2 \approx 0.5$ MeV. For nucleons, the rest-mass energy is $m_pc^2 \approx 1$ GeV. Because the total mass of the system is mostly due to the nucleons, the total rest-mass energy will be $E_{\rm mass} \cong NAm_pc^2 \cong Mc^2$, where $Am_p \simeq m$ is the mass of each nucleus and $Nm = M$ is the total mass of the system. Rest-mass energy is extensive – that is, $E_{\rm mass} \propto N$ – in the low-energy phenomena in which masses of individual nuclei do not change.

1.2.2 Atomic Binding Energies

If the particles of the system have internal structure (molecular, atomic, nuclear, etc.) then we get further energy scales that are characteristic of the interactions. The simplest is the atomic binding energy of atoms and molecules, which arises from the electromagnetic coupling between the particles.

The Hamiltonian describing an electron, moving in the Coulomb field of a nucleus of charge Zq, is given by $H_0 = (p^2/2m_e) - (Zq^2/r)$. If this electron is described by a wave function $\psi(\mathbf{x}, L)$, where L denotes the characteristic scale over which ψ varies significantly, then the expectation value for the energy of the electron in this state is $E(L) = \langle\psi|H_0|\psi\rangle \approx (\hbar^2/2m_eL^2) - (Zq^2/L)$. The first term arises from the fact that $\langle\psi|p^2|\psi\rangle = -\hbar^2\langle\psi|\nabla^2|\psi\rangle \approx (\hbar^2/L^2)$, which is equivalent to the uncertainty principle stated in the form $p \cong \hbar/L$. This expression for $E(L)$ reaches a minimum value of $E_{\min} = -Z^2\epsilon_a$ when L is varied, with the minimum occurring at $L_{\min} = (a_0/Z)$, where

$$a_0 \equiv \frac{\hbar^2}{m_e q^2} \equiv \frac{\lambda\!\!\!^{-}_e}{\alpha} \approx 0.52 \times 10^{-8} \text{ cm}, \quad \epsilon_a \equiv \frac{m_e q^4}{2\hbar^2} = \frac{1}{2}\alpha^2 m_e c^2 \approx 13.6 \text{ eV}, \tag{1.4}$$

with the definitions $\lambda\!\!\!^{-}_e \equiv (\hbar/m_e c)$ and $\alpha \equiv (q^2/\hbar c)$. a_0 and ϵ_a correspond to the size and the ground-state energy of a hydrogen atom with $Z = 1$. The wavelength λ corresponding to ϵ_a is $\lambda = (hc/\epsilon_a) = 2\alpha^{-2}\lambda\!\!\!^{-}_e \simeq 10^3$ Å and lies in the UV band. The fine-structure constant $\alpha \approx 7.3 \times 10^{-3}$ plays an important role in the structure of matter and arises as the ratio between several interesting variables:

$$\alpha = (v/Zc) = (2\mu_B/qa_0) = (r_0/\lambda\!\!\!^{-}_e) = (\lambda\!\!\!^{-}_e/a_0),$$

where v is the speed of an electron in the atom, $\mu_B \equiv (q\hbar/2m_e c)$ is the Bohr magneton representing the magnetic moment of the electron, and $r_0 \equiv (q^2/m_e c^2)$ is called the classical electron radius.

When atoms of size a_0 are closely packed, the number density of atoms is $n_{\text{solid}} \approx (2a_0)^{-3} \approx 10^{24}$ cm^{-3}. The binding energy of such a solid arises essentially because of the residual electromagnetic force between the atoms, and the typical binding energy per particle is $f\epsilon_a$ with $f \approx (0.1-1)$.

1.2.3 Molecular Binding Energy

The simplest molecular structure consists of two atoms bound to each other in the form of a diatomic molecule. The effective potential energy of interaction $U(r)$ between the atoms in such a molecule arises from a residual electrostatic coupling and has a minimum at a separation $r \simeq a_0$, approximately the size of the atom. The depth of the potential well at the minimum is comparable with the electronic-energy level ϵ_a of the atom. In addition to the internal, electronic, binding energies of the atoms comprising the molecule, there are two other contributions to the energy of a diatomic molecule:

(1) The atoms of such a molecule can vibrate at some characteristic frequency ω_{vib} about the mean position along the line connecting them; this will lead to vibrational-energy levels separated by $E_{\text{vib}} \approx \hbar\omega_{\text{vib}}$. If the displacement is $\sim a_0$ from the minimum, the vibrational energy E_{vib} will be $\sim \epsilon_a$. Writing $\epsilon_a \approx (1/2)\mu\omega_{\text{vib}}^2 a_0^2 \cong (\hbar^2/m_e a_0^2)$, where μ is the reduced mass of the two atoms, we get

$$E_{\text{vib}} = \hbar\omega_{\text{vib}} \approx \frac{\hbar^2}{(\mu m_e)^{1/2} a_0^2} \approx \left(\frac{m_e}{\mu}\right)^{1/2} \epsilon_a \simeq 0.25 \text{ eV} \tag{1.5}$$

if $\mu \simeq m_p$.

(2) The molecule can also rotate about an axis perpendicular to the line joining them. If the rotational angular momentum is J, this will contribute an energy of approximately

$$E_{\rm rot} \approx \left(\frac{J^2}{\mu a_0^2}\right) \approx \left(\frac{\hbar^2}{\mu a_0^2}\right) \approx \left(\frac{m_e}{\mu}\right)\epsilon_a \approx 10^{-3}\epsilon_a \simeq 10^{-2}\ \text{eV} \qquad (1.6)$$

if $J \simeq \hbar$ and $\mu \simeq m_p$. It follows from these relations that $E_{\rm rot}:E_{\rm vib}:E_0 \approx (m_e/\mu):(m_e/\mu)^{1/2}:1$ and $E_{\rm vib} \approx \sqrt{\epsilon_a E_{\rm rot}}$. Because $(m_e/\mu) \approx 10^{-3}$, the wavelengths of radiation from vibrational transitions are $\sim$40 times larger than those of electronic transitions; similarly, the rotational transitions lead to radiation with wavelengths $\sim$1000 times larger than those of electronic transitions. These wavelengths are usually in the IR band.

Atomic and molecular energies are also extensive, with the binding energy of a system of N particles scaling as N.

1.2.4 Nuclear-Energy Scales

Atomic nuclei are bound by the strong-interaction force that provides a binding energy per particle of $\sim$8 MeV, which is the characteristic scale for nuclear-energy levels. In the astrophysical context, a more relevant energy scale is the one at which nuclear reactions can be triggered in bulk matter, which can be estimated as follows. For two protons to fuse together while undergoing nuclear reaction, it is necessary that they be brought within the range of attractive nuclear force, which is approximately $l \approx (h/m_p c) = (2\pi\hbar/m_p c)$. Because this requires overcoming the Coloumb repulsion, such direct interaction can take place only if the kinetic energy of colliding particles is of the order of the electrostatic potential energy at the separation l. This requires energies of the order of $\epsilon \approx (q^2/l) = (\alpha/2\pi) m_p c^2 \approx 1$ MeV. It is, however, possible for nuclear reactions to occur through quantum-mechanical tunneling when the de Broglie wavelength $\lambda_{\rm deB} \equiv (h/m_p v) = l(c/v)$ of the two protons overlap. This occurs when the energy of the protons is approximately $\epsilon_{\rm nucl} \approx (\alpha^2/2\pi^2) m_p c^2 \approx 1$ keV. It is conventional to write this expression as $\epsilon_{\rm nucl} \approx \eta\alpha^2 m_p c^2$, with $\eta \simeq 0.1$. This quantity $\epsilon_{\rm nucl}$ sets the scale for triggering nuclear reactions in astrophysical contexts.

1.2.5 Gravitational Binding Energy

In the nonrelativistic, Newtonian theory for gravity, the gravitational energy of a system of size R and mass M will be $E_{\rm grav} \approx GM^2/R \approx (Gm_p^2/R)N^2$. This is not extensive with respect to N (for a given R), and the potential energy per particle varies as

$$\epsilon_g \equiv \frac{E_{\rm grav}}{N} = \left(\frac{Gm_p^2}{R}\right)N = \left(\frac{4\pi}{3}\right)^{1/3} Gm_p^2 N^{2/3} n^{1/3}, \tag{1.7}$$

where $n = (3N/4\pi R^3)$ is the number density of particles. The pressure due to gravitational force near the center of the object will be approximately

$$P_g \approx \frac{(GM^2/R^2)}{(4\pi R^2)} \approx \frac{1}{3}\left(\frac{4\pi}{3}\right)^{1/3} Gm_p^2 N^{2/3} n^{4/3} \cong \frac{1}{3}\left(\frac{E_{\rm grav}}{V}\right).$$

If the gravitational potential energy is comparable with the rest-mass energy of the system, it is necessary to take general relativistic effects into account. The ratio $\mathcal{R}_{gm} \equiv (E_{\rm grav}/E_{\rm mass})$ is $\mathcal{R}_{gm} \simeq 0.7(M/10^{33}\ {\rm gm})\,(R/1\ {\rm km})^{-1}$, which shows that if massive objects (with $M \simeq 10^{33}$ gm) are confined to small regions (with $R \simeq 1$ km), the system will exhibit general relativistic effects. When this ratio is small compared with unity, the system can be treated by Newtonian gravity.

1.2.6 Thermal and Degeneracy Energies of Particles

So far we have not introduced the notion of Temperature or the kinetic energy of the particle. These attributes bring in the next set of energy scales into the problem. For a particle of momentum p and mass m, the kinetic energy is given by

$$\epsilon = \sqrt{p^2c^2 + m^2c^4} - mc^2 = \begin{cases} p^2/2m & (p \ll mc) \\ pc & (p \gg mc) \end{cases}, \tag{1.8}$$

where the two forms are applicable in the non-relativistic (NR) and extreme relativistic (ER) limits. The behaviour of the system depends on the origin of the momentum distribution of the particles.

The familiar situation is the one in which short-range interactions (usually called ‘collisions’) between the particles effectively exchange the energy so as to randomize the momentum distribution. This will happen if the effective mean free path of the system l is small compared with the length scale L at which physical parameters change. (The explicit form taken by the condition $l \ll L$ can be very different in different cases; this condition is discussed in detail towards the end of this section.) When such a system is in steady state, we can assume that the local thermodynamic equilibrium, characterized by a local temperature T, exists in the system. Then the probability for occupying a state with energy E will scale as $P(E) \propto \exp[-(E/k_BT)]$. The typical momentum of the particle when the temperature is T is given by Eq. (1.8) with $\epsilon \simeq k_BT$, that is,

$$p \cong mc\left[\frac{2k_BT}{mc^2} + \left(\frac{k_BT}{mc^2}\right)^2\right]^{1/2} \cong \begin{cases} (2mk_BT)^{1/2} & (k_BT \ll mc^2;\ \text{NR}) \\ (k_BT/c) & (k_BT \gg mc^2;\ \text{ER}) \end{cases}. \tag{1.9}$$

In this case, the momentum and the kinetic energy of the particles vanish when $T \to 0$.

The situation is actually more complicated for material particles like electrons. The mean energy of a system of electrons will not vanish even at zero temperature because electrons obey the Pauli exclusion principle, which requires that the maximum number of electrons that can occupy any quantum state be two, one with spin up and another with spin down. Because the uncertainty principle requires that $\Delta x \Delta p_x \gtrsim h$, we can associate $(d^3 x d^3 p)/(2\pi\hbar)^3$ microstates with a phase-space volume $d^3 x\, d^3 p$. Therefore the number of quantum states with momentum less than p is $[V(4\pi p^3/3)/(2\pi\hbar)^3]$, where V is the spatial volume available for the system. The lowest energy state will be the one in which the N electrons fill all levels up to some momentum p_F, called Fermi momentum. This requires that

$$n = \left(\frac{N}{V}\right) = 2\frac{(4\pi p_F^3/3)}{(2\pi\hbar)^3} = \frac{1}{3\pi^2}\left(\frac{p_F}{\hbar}\right)^3, \tag{1.10}$$

giving $p_F = \hbar(3\pi^2 n)^{1/3}$. It is obvious that if $p_F \gtrsim mc$ the system must be treated as relativistic, even in the zero-temperature limit. The energy corresponding to p_F will be

$$\epsilon_F = \sqrt{p_F^2 c^2 + m^2 c^4} - mc^2 = \begin{cases} \dfrac{p_F^2}{2m} = \left(\dfrac{\hbar^2}{2m}\right)(3\pi^2 n)^{2/3} & \text{(NR)} \\ p_F c = (\hbar c)(3\pi^2 n)^{1/3} & \text{(ER)} \end{cases}. \tag{1.11}$$

The quantity ϵ_F (called the Fermi energy) sets the quantum-mechanical scale of the energy; quantum-mechanical effects will be dominant if $\epsilon_F \gtrsim k_B T$ (degenerate), and the classical theory will be valid for $\epsilon_F \ll k_B T$ (nondegenerate). The relevant ratio $\mathcal{R}_{\text{ft}} \equiv (\epsilon_F/k_B T)$ that determines that the degree of degeneracy is

$$\begin{aligned}\left(\frac{\epsilon_F}{k_B T}\right) &= \frac{mc^2}{k_B T}\left\{\left[\left(\frac{\hbar n^{1/3}}{mc}\right)^2 (3\pi^2)^{2/3} + 1\right]^{1/2} - 1\right\} \\ &\cong \begin{cases} \dfrac{1}{2}(3\pi^2)^{2/3}\left(\dfrac{\hbar^2}{m}\dfrac{n^{2/3}}{k_B T}\right) \\ (3\pi^2)^{1/3}\left(\dfrac{\hbar c}{k_B T} n^{1/3}\right) \end{cases},\end{aligned} \tag{1.12}$$

where the two limiting forms are valid for $n \ll (\hbar/mc)^{-3}$ (NR) and $n \gg (\hbar/mc)^{-3}$ (ER), respectively. In the first case $[n \ll (\hbar/m_e c)^{-3} \simeq 10^{31}\ \text{cm}^{-3}]$, the system is nonrelativistic; it will also be degenerate if $\mathcal{R}_{\text{ft}} = (\epsilon_F/k_B T) \gg 1$ and classical if $\mathcal{R}_{\text{ft}} \ll 1$. The transition occurs at $\mathcal{R}_{\text{ft}} \approx 1$, which corresponds to $nT^{-3/2} = [(mk_B)^{3/2}/\hbar^3] = 3.6 \times 10^{16}$ in cgs units. In the second case $[n \gg (\hbar/m_e c)^{-3} \simeq 10^{31}\ \text{cm}^{-3};\ \rho \equiv m_p n \gg 10^7\ \text{gm cm}^{-3}]$, electrons have $p_F \gg m_e c$ and are relativistic irrespective of temperature. The quantum effects will dominate thermal effects if $k_B T \ll (\hbar c)n^{1/3}$, and we will have a relativistic, degenerate gas.

In general, the kinetic energy of the particle will have contributions from the temperature as well as from Fermi energy. If we are interested in only the asymptotic limits, we can take the total kinetic energy per particle to be $\epsilon \approx \epsilon_F(n) + k_B T$. Note that such a system has a minimum energy $N\epsilon_F(n)$ even at $T = 0$.

By using our general result $P \simeq n\epsilon$ [see Eq. (1.3)], we can obtain the equation of state for the different cases discussed above. First, for a quantum-mechanical gas of fermionic particles with $k_B T \ll \epsilon_F$ and $\epsilon \approx \epsilon_F$, it follows from Eq. (1.11) that $P \simeq n\epsilon_F$ varies as the (5/3)rd power of density in the nonrelativistic case and as the (4/3)rd power of density in the relativistic case. Whether the system is relativistic or not is decided by the ratio (p_F/mc) or – equivalently – the ratio (ϵ_F/mc^2). The transition occurs at $n = n_{\rm RQ} \approx (\hbar/mc)^{-3}$. Second, if the system is classical with $k_B T \gg \epsilon_F$ so that $\epsilon \cong k_B T$, then $P \simeq nk_B T$ in both nonrelativistic and extreme relativistic limits.

The energy scale of the individual particles also characterizes the energy involved in the collisions between the particles. If this quantity is larger than the binding energy of the atomic system, the atoms will be ionised and the electrons will be separated from the atoms. The familiar situation in which this happens is at high temperatures with $k_B T \gtrsim \epsilon_a$ when the system will be made of free electrons and positively charged ions, whereas, if $k_B T \ll \epsilon_a$, the system will be neutral. The transition temperature at which nearly half the number of atoms are ionised occurs around $k_B T \approx (\epsilon_a/10)$, which is $\sim 10^4$ K for hydrogen. For $T \gg 10^4$ K, the kinetic energy of the free electrons in the hydrogen plasma will be $\sim k_B T$.

The electrons can be stripped off the atoms in another different context. This occurs if the matter density is so high that the atoms are packed close to each other, with the electrons forming a common pool with $\epsilon_F \gtrsim \epsilon_a$. In this case, the electrons will be quantum mechanical and the relevant energy scale for them will be ϵ_F. The temperature does not enter into the picture if $k_B T \ll \epsilon_F$, and we may call this a zero-temperature plasma. Conventionally, such systems are called degenerate. For normal metals in the laboratory the Fermi energy is comparable with the binding energy within an order of magnitude. If the temperature is below 10^4 K, the properties of the system are essentially governed by Fermi energy.

In the derivation of P in Eq. (1.3) it is assumed that the the gas is ideal, i.e., the mutual interaction energy of the particles is small compared with the kinetic energy. To treat a plasma as ideal, it is necessary that the Coulomb interaction energy of ions and electrons be negligible. The typical Coulomb potential energy between the ions and the electrons in the plasma is given by $\epsilon_{\rm Coul} \approx Zq^2 n^{1/3}$. If the classical high-temperature plasma is to be treated as an ideal gas, this energy should be small compared with the energy scale of the particle $\epsilon \approx k_B T$, which requires the condition $nT^{-3} \ll (k_B/Zq^2)^3 \simeq 2.2 \times 10^8 Z^{-3}$ in cgs units. On the other hand, to treat the high-density quantum gas as ideal, we should require that the Coulomb energy $\epsilon_{\mathrm{Coul}} \approx Zq^2n^{1/3}$ be small compared with the Fermi energy $\epsilon_F \approx (\hbar^2/2m)n^{2/3}$. The condition now becomes $n \gg 8Z^3a_0^{-3} \approx Z^3 \times 10^{26}\ \mathrm{cm}^{-3}$. Note that such a system becomes more ideal at higher densities; this is because the Fermi energy rises faster than the Coulomb energy.

Let us now go back to the tacit assumption we made in the above analysis, viz., that physical interactions between the particles of the system are capable of maintaining the thermal equilibrium. Determining the precise condition that will ensure this is not a simple task; but – naively – we would require that (1) the mean free path for particles, $l = (n\sigma)^{-1}$ based on a relevant scattering process governed by a cross section σ, be small compared with the scale L over which various parameters change significantly, and (2) that the mean time between collisions $\tau = (nv\sigma)^{-1}$ be small compared with the time scale over which physical parameters change.

To apply this condition we need to know the relevant mean free path for the system. For a neutral gas of molecules, this is essentially determined by molecular collisions with $\sigma_0 \approx \pi a_0^2 \approx 8.5 \times 10^{-17}\ \mathrm{cm}^2$ and $l = (n\sigma_0)^{-1}$. The time scale for the establishment of a Maxwellian distribution of velocities will be approximately $\tau_{\mathrm{neu}} \simeq l/v \propto n^{-1}T^{-1/2}$. For an ionized classical gas, the cross section for scattering is decided by Coulomb interaction between charged particles. Because an ionized plasma is made of electrons and ions with vastly different inertia, the interparticle collisions can take different time scales to produce thermal equilibrium between electrons, between ions, and between electrons and ions. Each of these needs to be discussed separately.

The typical impact parameter between two electrons is $b \approx (2Zq^2/m_ev^2)$, where v is the typical velocity of an electron. The corresponding e–e scattering cross section is

$$\sigma_{\mathrm{coul}} \approx \pi b^2 \approx \pi\left(\frac{Zq^2}{m_e}\right)^2 \frac{1}{v^4} \approx 10^{-20}\ \mathrm{cm}^2\ Z^2\left(\frac{T}{10^5\ \mathrm{K}}\right)^{-2}, \tag{1.13}$$

and the mean free path varies as $l = (n\sigma_{\mathrm{coul}})^{-1} \propto (T^2/n)$. The mean free time between the electron–electron scattering will be $\tau_{ee} \approx (n\sigma v)^{-1}$, where n is the number density of electrons and $\sigma \approx \pi b^2$. This gives $\tau_{ee} \approx (m_e^2v^3/2\pi Z^2q^4n)$, which is the leading dependence. (A more precise analysis changes the numerical coefficient and introduces an extra logarithmic factor; see Chap. 9.)

Note that $\tau \propto m^2v^3 \propto T^{3/2}m^{1/2}$ at a given temperature $T \propto (1/2)mv^2$. Therefore the ion–ion collision time scale τ_{pp} will be larger by the factor $(m_p/m_e)^{1/2} \simeq 43$, giving $\tau_{pp} = (m_p/m_e)^{1/2}\tau_{ee} \simeq 43\tau_{ee}$.

The time scale for significant transfer of energy between electrons and ions is still larger because of the following fact. When two particles (of unequal mass) scatter off each other, there is no energy exchange in the centre-of-mass frame. In the case of ions and electrons, the centre-of-mass frame differs from the lab frame only by a velocity $v_{\mathrm{CM}} \simeq (m_e/m_p)^{1/2}v_p \ll v_p$. Because there is no energy exchange in the centre-of-mass frame, the maximum energy transfer in the lab frame (which occurs for a head-on collision) is approximately $\Delta E = (1/2)m_p(2v_{\rm cm})^2 = 2m_p v_{\rm cm}^2 \simeq 2m_e v_p^2$, giving $[\Delta E/(1/2)m_p v_p^2] \simeq (m_e/m_p) \ll 1$. Therefore it takes (m_p/m_e) times more collisions to produce equilibrium between electrons and ions, that is, the time scale for electron–ion collision is $\tau_{pe} = (m_p/m_e)\tau_{ee} \simeq 1836\tau_{ee}$. The plasma will relax to a Maxwellian distribution in this time scale.

Finally, it must be noted that in a high-temperature tenuous plasma, this mean free path can become larger than the size of the system. If that happens, it is necessary to check whether there are any other physical processes that can provide an effective mean free path that is lower. Most astrophysical plasmas host magnetic fields that make the charged particles spiral around the magnetic-field lines. We can estimate the typical radius of a spiraling charged particle in a magnetic field by equating the centrifugal force (mv^2/r) to the magnetic force (qvB/c). This leads to a radius called the Larmor radius, given by

$$r_L = (mcv/qB) = 13 \text{ cm } (T/10^5 \text{ K})^{1/2}(B/1 \text{ G})^{-1}$$

in a thermal plasma. When the Larmor radius is small, it can act as the effective mean free path for the scattering of charged particles. The ratio between the mean free path from Coulomb collisions $[l \propto (T^2/n)]$ and the Larmor radius $[r_L \propto (T^{1/2}/B)]$ varies as $(BT^{3/2}/n)$ and can be large in tenuous high-temperature plasmas with strong magnetic fields. This ratio is unity for a critical magnetic field:

$$B_c = 10^{-19} \text{ G}\left(\frac{T}{10^5 \text{ K}}\right)^{-3/2}\left(\frac{n}{1 \text{ cm}^{-3}}\right). \tag{1.14}$$

The magnetic field in most astrophysical plasmas will be larger than B_c, and hence this effect will be important.

1.3 Classical Radiative Processes

We next turn to the question of gathering information about the cosmic structures from the radiation received from them. To relate the information received through the electromagnetic waves to the properties of the emitting system, it is necessary to understand the process of electromagnetic radiation from different systems and the nature of the spectrum emitted by each of them.

In classical electromagnetic theory, radiation is emitted by any charged particle that is in accelerated motion. A detailed argument given in Chap. 3 shows that the total amount of energy radiated per second in all directions by a particle with charge q moving with acceleration a is given by

$$\frac{d\mathcal{E}}{dt} = \frac{2}{3}\frac{q^2}{c^3}a^2, \tag{1.15}$$

provided the acceleration is measured in the frame in which the particle is instanteneously at rest. The rate of energy emission, of course, is independent of the frame used to define it. This result is called Larmor's formula and can be used to understand a host of classical electromagnetic phenomena. Because $\mathbf{d} = (q\mathbf{x})$ is the dipole moment related to an isolated charge located at position $\mathbf{x}$, this formula shows that the total power radiated is proportional to the square of $\ddot{\mathbf{d}}$. In bounded motion, if $\mathbf{d}$ varies at frequency ω (so that $\ddot{\mathbf{d}} = -\omega^2\mathbf{d}$), then the energy radiated is given by

$$\frac{d\mathcal{E}}{dt} = \frac{2}{3}\frac{d^2}{c^3}\omega^4. \tag{1.16}$$

Different physical phenomena are essentially characterised by different sources of acceleration in Eq. (1.15) for the charged particle. Let us consider two specific examples.

1.3.1 Thermal Bremsstrahlung

As a first example consider a scattering between an electron of mass m_e and a proton, with an impact parameter b and relative velocity v in a hydrogen plasma. The acceleration of the electron is $a \approx (q^2/m_e b^2)$ and lasts for a time (b/v). Such an encounter will result in the radiation of energy $\mathcal{E} \approx (q^2 a^2/c^3)(b/v) \approx (q^6/c^3 m_e^2 b^3 v) \approx (q^6 n_i/c^3 m_e^2 v)$, as $b \approx n_i^{-1/3}$ on the average. The total energy radiated per unit volume will be $n_e\mathcal{E}$. Because each collision lasts for a time (b/v), there will be very little radiation at frequencies greater than (v/b). For $\omega < (v/b)$, we may take the energy emitted per unit frequency interval to be nearly constant. Further, in the case of plasma in thermal equilibrium, $v \cong (k_B T/m_e)^{1/2}$. Putting all these together, we get

$$j_\omega \equiv \left(\frac{d\mathcal{E}}{d\omega\, dt\, dV}\right) \simeq \left(\frac{q^6}{m_e^2 c^3}\right)\left(\frac{m_e}{k_B T}\right)^{1/2} n_e n_i \propto n^2 T^{-1/2}; \quad (\text{for } \hbar\omega \lesssim k_B T). \tag{1.17}$$

This process is called thermal bremsstrahlung. The bremsstrahlung spectrum is flat for $0 < \omega \lesssim (k_B T/\hbar)$ and will fall rapidly for $\omega \gtrsim (k_B T/\hbar)$, where the upper limit comes from the fact that an electron with a typical energy of $(k_B T)$ cannot emit photons with energy higher than $k_B T/\hbar$. The total energy radiated, over all frequencies, from such a plasma can be found by integration of this expression over ω in the range $(0, k_B T/\hbar)$. This gives

$$\left(\frac{d\mathcal{E}}{dt\, dV}\right) = \int_0^{(k_B T/\hbar)} d\omega \left(\frac{d\mathcal{E}}{d\omega\, dt\, dV}\right) \simeq \left(\frac{q^6}{m_e^2 c^3}\right)\left(\frac{m_e k_B T}{\hbar^2}\right)^{1/2} n_e n_i. \tag{1.18}$$

1.3.2 Synchrotron Radiation

Another major source of acceleration for charged particles is the magnetic fields hosted by plasmas. This process, called synchrotron radiation, can be estimated as follows: Consider an electron moving with velocity **v** in a magnetic field **B**. To use Eq. (1.15) we need to estimate the acceleration in the instantaneous rest frame of the particle. In that frame, the magnetic force $(q/c)[\mathbf{v}\times\mathbf{B}]$ is zero, but the magnetic field in the lab frame will lead to an electric field of magnitude $E' \simeq \gamma B$ (see Chap. 3) in the instantaneous rest frame of the charge, inducing an acceleration $a' = (qE'/m_e)$. Accelerated by this field, the charged particle will radiate energy at the rate (which is the same in the rest frame and in the lab frame)

$$\frac{d\mathcal{E}}{dt} = \left(\frac{d\mathcal{E}'}{dt'}\right) = \frac{2}{3}\frac{q^2}{c^3}(a')^2 = \frac{2}{3}\frac{q^2}{c^3}\left(\frac{q^2}{m_e^2}\gamma^2 B^2\right). \tag{1.19}$$

The power radiated by an electron of energy $\epsilon = \gamma m_e c^2$ is $(d\mathcal{E}/dt) \propto \epsilon^2 B^2$. Further, the energy density in the magnetic field is $U_B = (B^2/8\pi)$; hence we can write

$$\left(\frac{d\mathcal{E}}{dt}\right) = \frac{16\pi}{3}\left(\frac{q^2}{m_e c^2}\right)^2 \gamma^2 c U_B \simeq (\sigma_T c U_B)\gamma^2, \tag{1.20}$$

where $\sigma_T \equiv (8\pi/3)(q^2/m_e c^2)^2$ is called the Thomson scattering cross section.

For a nonrelativistic particle spiralling in a magnetic field, the characteristic angular frequency is $\omega = (r_L/v) = (qB/m_e c)$. For relativistic motion with constant v^2, the effective mass is $m_e(1 - v^2/c^2)^{-1/2} = m_e\gamma$, so that the angular frequency becomes $\omega = (qB/mc\gamma) = (qcB/\epsilon)$ for a particle of energy ϵ in a magnetic field of strength B; the synchrotron radiation from an extreme relativistic particle will peak at the frequency

$$\omega_c \approx \omega\gamma^3 \propto B\gamma^2 \propto B\epsilon^2, \tag{1.21}$$

where the extra factor γ^3 arises from special relativistic effects (see Chap. 3). One factor of γ arises from time dilation; the other factor of γ^2 arises from a Doppler factor $[1 - (v/c)]^{-1} \approx 2\gamma^2$ in the $v \to c$ limit.

The total radiation emitted from a bunch of particles will be $j_\omega \propto (B^2\epsilon^2)[n(\epsilon)]$ $(d\epsilon/d\omega)$, where the first factor, $B^2\epsilon^2$, is the energy emitted by a single particle, the second factor is the number of particles with energy ϵ, and the last factor is the Jacobian $(d\epsilon/d\omega) \propto \epsilon^{-1} \propto \omega^{-1/2}$ from ϵ to ω. If the spectrum of particles is a power law $n(\epsilon) = C\epsilon^{-p}$, then the radiation spectrum will be

$$j_\nu \approx \frac{e^3}{m_e c^2}\left(\frac{3e}{4\pi m_e^3 c^5}\right)^{(p-1)/2} C B^{(p+1)/2}\nu^{-(p-1)/2}, \tag{1.22}$$

where we have reintroduced all the constants. (A more precise calculation multiplies the expression by a p-dependent factor, which is $\sim$0.1.) This leads to a power-law spectrum, $j_\nu \propto \nu^{-\alpha}$ with $\alpha = (p-1)/2$.

1.4 Radiative Processes in Quantum Theory

The radiation field in quantum theory is described in terms of photons, and the emission or absorption of radiation arises when a physical system makes the transition from one energy level to another. We have already determined the main energy levels of atoms and molecules in Subsection 1.2.2. The transition between these energy levels in an atom will correspond to photon energies upwards of few electron volts, and the corresponding wavelength will be in optical and UV bands in most of the cases.

This estimate of atomic-energy levels was, however, based on the simple form of the Hamiltonian for the electron in an atom. The actual Hamiltonian is a lot more complicated than H_0 used in Subsection 1.2.2. The corrections to H_0 lead to splitting of the original energy levels and allow emission of photons of widely different frequencies by the atomic system. We now consider these corrections.

1.4.1 Fine Structure and Hyperfine Structure

The Hamiltonian for an electron in a hydrogen atom can be expressed as a sum, $H \cong H_0 + H_{\rm rel} + H_{\rm sp-or} + H_{\rm sp-sp}$, where $H_0 = (p^2/2m_e) - (Zq^2/r)$ is the original (zeroth-order) Hamiltonian and the rest are lowest-order corrections. The first correction $H_{\rm rel} = -(p^4/8m_e^3c^2)$ is the relativistic correction to the kinetic energy $p^2/2m_e$ that arises as the second term in the Taylor series expansion of $\epsilon(p)$ in Eq. (1.8); the correction $H_{\rm sp-or}$ arises from the coupling between the spin magnetic moment of the electron $\mu_e \simeq (q\hbar/2m_ec)$ and the magnetic field $B \cong (v/c)E \cong (v/c)(Zq/r^2)$ in the instantaneous rest frame of the electron, obtained by transformation of the Coulomb field. This should have the magnitude

$$\bar{H}_{\rm sp-or} = \mu B = \frac{Zq^2}{2r^2}\frac{\hbar v}{m_ec^2} = \frac{Zq^2}{m_e^2c^2r^3}(\mathbf{l}\cdot\mathbf{s}), \tag{1.23}$$

where $\mathbf{l}$ and $\mathbf{s}$ are the orbital and the spin angular momenta of the electron. The actual result is half of this value where the extra factor arises due to a phenomenon called Thomas precession, to be discussed in Chap. 3, exercise 3.4. The next correction,

$$H_{\rm sp-sp} = \boldsymbol{\mu}_e \cdot \left(\frac{\boldsymbol{\mu}_N}{r^3} - \frac{3\mathbf{r}\cdot\boldsymbol{\mu}_N}{r^5}\mathbf{r}\right), \tag{1.24}$$

is the coupling between the nuclear magnetic moment and the magnetic moment of the electron. These magnetic moments are given by

$$\begin{aligned} \boldsymbol{\mu}_e &= -\left[2 + \frac{\alpha}{\pi} + \mathcal{O}(\alpha^2)\right]\frac{q\hbar}{2m_ec}\mathbf{s} \equiv -g_e\mu_B\mathbf{s}; \\ \boldsymbol{\mu}_p &\simeq 5.6\left(\frac{q\hbar}{2m_pc}\right)\mathbf{S} \equiv g_N\mu_N\mathbf{S}, \end{aligned} \tag{1.25}$$

where $\mu_B = (q\hbar/2m_e c)$ is called the Bohr magneton, μ_N is the corresponding quantity for the proton, and **s** and **S** are the spin vectors of electron and proton, respectively.

It is now easy to evaluate the order of magnitude of these corrections. The zeroth-order term H_0 is of the order of $(q^2/a_0) \approx 10$ eV, corresponding to $\lambda \simeq$ 1200 Å. The first correction gives

$$\frac{p^4}{m_e^3 c^2} \approx \frac{p^2}{m_e}\left(\frac{p}{m_e c}\right)^2 \approx \left(\frac{v}{c}\right)^2 \frac{q^2}{a_0} \approx \alpha^2 E_0 \approx 10^{-3} \text{ eV}, \tag{1.26}$$

with the corresponding photon wavelength of $\lambda \simeq 1$ mm. The second correction, with $l \simeq s \simeq \hbar$, is

$$\frac{q^2\hbar^2}{m_e^2 c^2 a_0^3} \approx \frac{q^2}{a_0}\left(\frac{\hbar}{m_e c a_0}\right)^2 \approx \alpha^2 E_0, \tag{1.27}$$

which is of the same order as that of the first correction. These two together are called fine-structure corrections. The third correction is of the order of

$$\frac{\mu_B \mu_N}{a_0^3} \approx \frac{m_e}{m_p}\frac{\mu_B^2}{a_0^3} \approx \frac{m_e}{m_p}\left(\frac{\hbar}{m_e c a_0}\right)^2 \frac{q^2}{a_0} \approx 10^{-3}\alpha^2 E_0 \approx 10^{-6} \text{ eV}, \tag{1.28}$$

(corresponding to $\lambda \simeq 10^2$ cm), which is smaller and is called the hyperfine correction. A more precise calculation gives the wavelength of radiation emitted in the hyperfine transition of hydrogen to be $\sim$21 cm. This radiation, which is in the radio band, is used extensively in astronomy as a diagnostic of atomic (neutral) hydrogen.

1.4.2 Transition Rates and Cross Sections

To complete the quantum-mechanical analysis, we also need to estimate the rate of transition between the various levels. Consider an initial state with an atom in ground state $|G\rangle$ and n photons present. Absorbing a photon, the atom makes the transition to the excited state $|E\rangle$, leaving behind an $(n-1)$ photon state. Let the probability for this process be $\mathcal{P}[|G\rangle|n\rangle \to |E\rangle|n-1\rangle] \propto n \equiv Qn$. The fact that this absorption probability $\mathcal{P}$ is proportional to n seems intuitively acceptable. Consider now the probability $\mathcal{P}'$ for the time-reversed process $[|E\rangle|n-1\rangle \to |G\rangle|n\rangle]$. By principle of microscopic reversibility, we expect $\mathcal{P}' = \mathcal{P}$, giving $\mathcal{P}' \propto n \equiv Qn$. Calling $n-1 = m$, we get $\mathcal{P}'[|E\rangle|m\rangle \to |G\rangle |m+1\rangle] = Qn = Q(m+1)$. Clearly $\mathcal{P}'$ is nonzero even for $m = 0$; $\mathcal{P}'[|E\rangle|0\rangle \to |G\rangle|1\rangle] = Q$, which gives the probability for a process conventionally called spontaneous emission. The term Qm gives the corresponding probability for stimulated emission. Thus the fact that absorption probabilities are proportional to n whereas emission probabilities are proportional to $n+1$ originates from the principle of microscopic reversibility.

The basic rate, governed by Q, can be estimated by use of the correspondence with classical theory. If the rate of transition between two energy levels is Q and the energy of the photon emitted during the transition is $\hbar\omega$, then the rate of energy emission is $Q\hbar\omega$. Classically, the same system will emit energy at the rate $(d^2\omega^4/c^3)$, where d is the electric dipole moment of the atom. (This assumes that the radiation is predominantly due to direct coupling between the radiation and the dipole moment of the atom; if not, we have to use the relevant moment – like the electric quadrupole moment or magnetic dipole moment, instead of d – in this equation.) Writing $Q\hbar\omega \approx (d^2\omega^4/c^3)$, we find that

$$Q \cong \frac{\omega^3 d^2}{\hbar c^3} \simeq \frac{\alpha^5}{8}\left(\frac{\lambda\!\!\!^{-}}{c}\right)^{-1} \simeq \frac{\alpha^5}{8}\left(\frac{m_e c^2}{\hbar}\right) \approx 10^9\ \mathrm{s}^{-1}, \tag{1.29}$$

where we have used $d = qa_0 \simeq (q\lambda\!\!\!^{-}_e/\alpha)$ and $\hbar\omega \simeq (1/2)\alpha^2\, m_e c^2$. The rate Q can also be expressed in different forms as

$$Q \approx \frac{q^2}{\hbar c}\frac{a_0^2}{c^2}\omega^3 = \frac{q^2}{m_e c^3}\omega^2 = \omega^2\frac{r_0}{c}, \tag{1.30}$$

where $r_0 = (q^2/m_e c^2)$ is the classical electron radius. A more precise quantum-mechanical calculation corrects this by contributing an extra numerical factor f (called oscillator strength).

The transition rate for other processes, such as the 21-cm radiation, can be estimated in the same manner by using Eq. (1.16). In the relation $Q\hbar\omega_{21} \approx (\omega_{21}^4 d^2/c^3)$, we now have to use the magnetic dipole moment of electron $d \approx (q\hbar/m_e c)$. This gives $Q \approx \alpha(\lambda\!\!\!^{-}_e/c)^2\omega_{21}^3$. Estimating $\hbar\omega_{21}$ from expression (1.28) derived above for the hyperfine-structure energy level, we can evaluate this transition rate as

$$Q_{21\mathrm{cm}} \simeq \left(\frac{r_0\omega_{21}}{c}\right)\left(\frac{\hbar\omega_{21}}{m_e c^2}\right)\omega_{21} \approx 10^{-15}\ \mathrm{s}^{-1}. \tag{1.31}$$

The ratio between this rate and the transition rate between the primary energy levels of the hydrogen atom computed in relation (1.29) is

$$\frac{Q_{21\mathrm{cm}}}{Q} \simeq \left(\frac{\omega_{21}}{\omega}\right)^3\left(\frac{\lambda\!\!\!^{-}_e}{a_0}\right)^2 \approx 10^{-24}. \tag{1.32}$$

Clearly, hyperfine transitions are very slow processes.

This analysis also shows that every excited state has a probability of decaying spontaneously to the ground state with a decay rate Q. Hence the lifetime Δt of the excited state is approximately

$$\Delta t \approx Q^{-1} \approx \left(\frac{q^2}{\hbar c}\right)^{-1}\left(\frac{a_0}{\lambda\!\!\!^{-}}\right)^{-2}\omega^{-1} \approx \left(\frac{10^8}{\omega}\right) \approx 10^{-9}\ \mathrm{s} \tag{1.33}$$

for optical radiation. (It is correspondingly larger and is approximately $\Delta t = Q_{21\text{ cm}}^{-1} \simeq 10^{15}$ s for 21-cm radiation.) From the uncertainty principle between the energy and time, it follows that the energy level of the excited state will be uncertain by an amount ΔE of the order of $(\hbar/\Delta t) \approx \hbar Q$. In the absence of such an uncertainty, the transition between the two energy levels could lead to infinitely sharp spectral lines at a specific frequency ω. The width of the excited states leads to a corresponding width to the spectral line called the natural width $\Delta\omega$, where $(\Delta\omega/\omega) = (Q/\omega) \approx 10^{-8}$ for the main hydrogen lines. In terms of wavelength, the natural width $\Delta\lambda = 2\pi c(\Delta\omega/\omega^2)$ is of the order of the classical electron radius: $\Delta\lambda \approx 2\pi r_0$.

Because of the finite linewidth, it is convenient to introduce a (frequency-dependent) bound–bound cross section $\sigma_{bb}(\omega)$ for the absorption of radiation by the system, which is sharply peaked at $\omega = \omega_0$ with a width of $\Delta\omega$. If the phase-space density of photons is $dN = n[d^3x d^3p/(2\pi\hbar)^3]$, then the number density of photons per unit volume participating in the absorption is $\mathcal{N} = nd^3p/(2\pi\hbar)^3 = (n\omega_0^2/\pi c^3)(\Delta\omega/2\pi)$. The corresponding flux is $\mathcal{N}c$, and the rate of absorption is

$$\mathcal{N}\sigma_{bb}c = \frac{n\omega_0^2}{\pi c^2}\sigma_{bb}\frac{\Delta\omega}{2\pi} = Qn = \omega_0^2\left(\frac{r_0}{c}\right)n, \tag{1.34}$$

giving $\sigma_{bb}(\Delta\omega/2\pi) = \pi r_0 c$. This result can be stated more formally as

$$\int_0^\infty \sigma_{bb}(\omega)\frac{d\omega}{2\pi} = \pi r_0 c = \frac{\pi q^2}{m_e c} = \left(\pi r_0^2\right)\left(\frac{c}{r_0}\right); \quad r_0 \equiv \left(\frac{q^2}{m_e c^2}\right) \tag{1.35}$$

which suggests expressing the cross section as

$$\sigma_{bb}(\omega) \equiv \frac{\pi q^2}{m_e c}\phi_\omega, \tag{1.36}$$

where ϕ_ω is called the line-profile function; the integral of ϕ_ω over $(d\omega/2\pi)$ is unity. When the linewidths are ignored, ϕ_ω is proportional to the Dirac delta function; when the finite width of the energy levels is taken into account, ϕ_ω will become a function that is peaked at ω_0 with a narrow width $\Delta\omega$, such that $\phi(\omega_0) \cong (\Delta\omega)^{-1}(2\pi)$. The absorption cross section at the centre of the line $\omega = \omega_0$ is given by $\sigma \simeq 2\pi^2(rc/\Delta\omega) \simeq (\lambda_0^2/2)$, where λ_0 is the wavelength of the photon. A more rigorous quantum-mechanical theory will provide the explicit form for $\phi(\omega)$ (which turns out to be a Lorentzian in this case) and an overall multiplicative factor f called the oscillator strength.

1.4.3 Thermal Radiation

The result regarding the emission and the absorption rates also allows us to determine the the energy distribution of photons in equilibrium with matter at temperature T. In such a situation, photons will be continuously absorbed and emitted by matter. Consider the rate of absorption (or emission) of photons between any two levels, say, a ground state $|G\rangle$ and an excited state $|E\rangle$. We saw above that the absorption rate per atom is given by Qn and the emission rate is $Q(n+1)$, where n is the number of photons present and Q is determined from the quantum theory of radiation. In steady state, the number of upward and downward transitions must match, which requires that product (number of atoms in G) $\times$ (rate of upward transitions per atom) equal (number of atoms in E) $\times$ (rate of downward transitions per atom), that is, $N_G Qn = N_E Q(n+1)$. Because matter is in thermal equilibrium at temperature T, we must also have $(N_E/N_G) = \exp(-\Delta E/k_B T)$, where ΔE is the energy difference between the two levels. This relation should hold for all forms of matter with arbitrary energy levels; hence we can take the ground-state energy to be zero (i.e, arbitrarily small) and the excited-state energy to be E, leading to

$$n = \frac{1}{(N_G/N_E) - 1} = \frac{1}{\exp(E/k_B T) - 1}. \tag{1.37}$$

This equation gives the number of photons with energy E [or – equivalently – with momentum $p = (E/c)$] in thermal equilibrium with matter. To be more precise, the number of photons with momentum in the interval $[\mathbf{p}, \mathbf{p} + d^3\mathbf{p}]$ is given by $dN = 2n[V d^3 p/(2\pi\hbar^3)]$, where the factor in the square brackets gives the number of quantum states in the phase volume $V d^3 p$ and the factor 2 takes into account the two spin states for each photon. The corresponding energy dE flowing through $d^3 x = dA(cdt)$ will be $dE = h\nu\, dN = 2n(\nu)h\nu\, dA[cdt][d^3 p/h^3]$. Writing $d^3 p = p^2 dp\, d\Omega = (h/c)^3 \nu^2\, d\nu\, d\Omega$, we can determine the intensity (which is the energy per unit area per unit time per solid angle per frequency) of thermal radiation as

$$\frac{dE}{dA\, dt\, d\Omega\, d\nu} \equiv B_\nu = \frac{2h\nu^3}{c^2} n(\nu) = \frac{2h\nu^3}{c^2} \frac{1}{e^{h\nu/k_B T} - 1}. \tag{1.38}$$

The quantity νB_ν reaches a maximum value around $h\nu \approx 4k_B T$, which translates to the fact that a blackbody at 6000 K will have the maximum for νB_ν at 6000 Å. The maximum intensity is $(\nu B_\nu)_{\max} \approx (T/100\text{ K})^4\ \text{W m}^{-2}\ \text{sr}^{-1}$. Such thermal radiation can arise in many different contexts in which a primary source of energy is thermalised because of some physical process, the most important example being stellar radiation.

At low frequencies, the intensity of thermal radiation given by Eq. (1.38) will be $B_\nu \approx (2k_B T/\lambda^2)$. Because of this relation, it is conventional to define a brightness temperature for any source with intensity I_ν as $T_B \equiv (\lambda^2 I_\nu/2k_B)$, which is (in general) a function of frequency.

It is clear from Eq. (1.37) that there are very few photons with momentum greater than $\bar{p} \approx (k_B T/c)$, so that $(N/V) \approx (4\pi/3)(\bar{p}/2\pi\hbar)^3 \approx (k_B T/\hbar c)^3$ and the mean energy is $U_{\text{ER}} \approx k_B T(N/V) \approx (k_B T)^4/(\hbar c)^3$.

1.4.4 Photon Opacities in Matter

Let us next determine the conditions under which our original assumption – that the radiation is in thermal equilibrium with matter – holds. If the cross section for the relevant process that scatters or absorbs radiation is given by σ and the number density of scatterers is n, then the mean free path of a photon is given by $l = (n\sigma)^{-1}$. In the case of radiation, it is conventional to define a quantity κ (called opacity) such that

$$\alpha \equiv n\sigma \equiv \rho\kappa, \tag{1.39}$$

where ρ is the mass density of the scatterers. The optical depth of a system of size R is defined to be $\tau \equiv \alpha R = (R/l)$. From the standard theory of random walk, we know that a photon will traverse a distance R with N_c collisions, where $R = N_c^{1/2} l$; that is, the number of collisions is given by $N_c = (R/l)^2 = \tau^2$, provided that $\tau \gg 1$.

The opacity for the photons is provided mainly by three different processes: (1) scattering by free electrons, (2) the free–free absorption of photons, and (3) the bound–free transitions induced in matter by the photons that are passing through it.

(1) The simplest case is the one in which the charged particle is accelerated by an electromagnetic wave that is incident upon it. Consider a charge q placed on an electromagnetic wave of amplitude E. The wave will induce an acceleration $a \simeq (qE/m)$, causing the charge to radiate. The power radiated will be $P = (2q^2a^2/3c^3) = (2q^4/3m^2c^3)E^2$. Because the incident power in the electromagnetic wave is $S = (cE^2/4\pi)$, the scattering cross section (for electrons with $m = m_e$) is

$$\sigma_T \equiv \frac{P}{S} = \frac{8\pi}{3}\left(\frac{q^2}{m_e c^2}\right)^2 \approx 6.7 \times 10^{-25}\ \mathrm{cm}^2, \tag{1.40}$$

which is the Thomson scattering cross section. This cross section governs the basic scattering phenomena between charged particles and radiation. The corresponding mean free path for photons through a plasma is $l_T = (n_e\,\sigma_T)^{-1}$, and the Thomson scattering opacity, defined to be $\kappa_T \equiv (n_e\sigma_T/\rho)$, is

$$\kappa_T = \left(\frac{n_e}{n_p}\right)\left(\frac{\sigma_T}{m_p}\right) = 0.4\ \mathrm{cm}^2\ \mathrm{gm}^{-1} \tag{1.41}$$

for ionised hydrogen with $n_e = n_p$.

The opacity for the process in (2) and (3) can be determined by the principle of detailed balance which allows us to relate the rate for certain processes to the rate for the corresponding 'inverse' process.

(2) The time-reversed process corresponding to bremsstrahlung is the one in which a photon is absorbed by an electron while in the proximity of an ion.

In equilibrium, the rate for this free–free absorption should match that of thermal bremsstrahlung. We write the free–free absorption rate as $n\sigma_{ff}B(\nu)$, where σ_{ff} is the free–free absorption cross section and $B(\nu) \propto \nu^3(e^{\hbar\nu/k_BT} - 1)^{-1} \propto \nu^2 T$ (when $\hbar\nu \ll k_BT$) is the intensity of the thermal radiation. Equating this to the bremsstrahlung emissivity found in Eq. (1.17), $j_\nu \propto n^2T^{-1/2}$, we get $\sigma_{ff} \propto (n/\nu^2T^{3/2})$. Taking the typical frequency of the photon to be proportional to T, we find that $\sigma_{ff} \propto nT^{-3.5}$. The corresponding opacity can be written in the form

$$\kappa_{ff} \propto \rho T^{-3.5}. \tag{1.42}$$

(3) To obtain the bound–free opacity, which arises when a photon ionizes an atom, we begin by relating the photoionization rate to the recombination rate in which an ion and an electron get bound together, releasing the excess energy as radiation. The recombination rate per unit volume of a plasma will be proportional to (1) the number density of electrons n_e, (2) the number density of ions n_i, (3) the relative velocity of encounter v, and (4) the cross section for the process, which will be $\sim\pi\lambda^2$, where λ gives the effective range of interaction between electron and proton. For Coulomb interaction, this range is $\lambda_1 \cong (2Zq^2/m_ev^2)$; on the other hand, an electron of speed v has a de Broglie wavelength of $\lambda_2 \cong (\hbar/m_ev)$. We should choose λ to be the larger of λ_1 or λ_2, depending on the context. Let us first consider the case with $\lambda \simeq \lambda_2$, which corresponds to $(v/c) \gtrsim (q^2/\hbar c)$. Each recombination will release an energy of approximately $(1/2)m_ev^2$. Hence,

$$\left(\frac{dE_{\rm rec}}{dV\,dt}\right) \propto \left(\frac{m_ev^2}{2}\right)(n_en_i)\left(\frac{h}{m_ev}\right)^2 v \propto n_en_iT^{1/2} \propto \rho^2T^{1/2}, \tag{1.43}$$

where we have assumed that $m_ev^2 \approx k_BT$, $n_e \propto \rho$, and $n_i \propto \rho$. In equilibrium, the photoionisation rate (which removes energy from the radiation field) should match the recombination rate. The amount of energy removed by photoionisation is proportional to $dE_{\rm ion} \propto n_{\rm atom}\sigma_{bf}E_{\rm rad}$, where σ_{bf} is the photoionisation cross section. Equating $dE_{\rm ion}$ to $dE_{\rm rec}$ and using $E_{\rm rad} \propto T^4$, we get

$$n_{\rm atom}\sigma_{bf}T^4 \propto n_en_iT^{1/2}. \tag{1.44}$$

Introducing the bound–free opacity κ_{bf} by the definition $\kappa_{bf} = (n_{\rm atom}\sigma_{bf}/\rho)$ and taking $n_e \propto \rho$ and $n_i \propto \rho$, we find that

$$\kappa_{bf} \propto \rho T^{-3.5} \tag{1.45}$$

which scales just like relation (1.42).

In a radiation bath with temperature T, the typical energy of photons is $h\nu \simeq k_BT$. The result of relation (1.45) suggests that the frequency dependence of $\sigma_{bf}(\nu) \propto \kappa_{bf} \propto T^{-3.5}$ will be of the form $\sigma(\nu) = \sigma_{bf}(\nu/\nu_I)^{-s}$ for $\nu > \nu_I$ (and zero otherwise). Here $s \approx 3$–3.5 and $\nu_I = (\epsilon_a/h)$ is the frequency corresponding to the ionisation energy ϵ_a of the atom. Because the cross section for photoionisation $\sigma(\nu)$ satisfies constraint (1.35),

$$\int_0^\infty \sigma(\nu)\,d\nu = \pi r_0 c f = \left(\frac{\pi e^2}{m_e c}\right) f, \tag{1.46}$$

where the term within the parentheses comes from classical theory and the oscillator strength f is supplied by the quantum theory, we get

$$\sigma_{bf} = \pi(s-1) f r_0 \lambda_I \simeq 2\pi f r_0 \lambda_I, \tag{1.47}$$

where $\lambda_I = (c/\nu_I)$ and $s \simeq 3$. This shows that the photoionisation cross section is essentially the product of the classical electron radius and the wavelength at ionisation threshold. Using $\lambda_I = 912$ Å, we get $\sigma_{bf} \approx 10^{-17}$ cm^2 for hydrogen. For heavier elements σ_{bf} will scale as

$$\sigma(\nu) = \sigma_{bf}\left(\frac{\nu_I}{\nu}\right)^3 \propto f r_0 \left(\frac{c}{\nu_I}\right)\left(\frac{\nu_I}{\nu}\right)^3 \propto \left(\frac{\nu_I^2}{\nu^3}\right) \propto Z^4 \nu^{-3} \tag{1.48}$$

if we take $s = 3$.

The cross section for recombination, σ_{rec}, is related to σ_{bf} by $4\sigma_{\text{rec}} d^3 p_e = 8\sigma_{bf} d^3 p_\gamma$ where $4 = 2 \times 2$ is due to electron and proton spins, $8 = 2 \times 2 \times 2$ is due to electron, proton, and photon spins, and p_e and p_γ refer to the momenta of the electron and the photon, respectively. Because $dp_e \simeq dp_\gamma$, this gives $\sigma_{\text{rec}} = 2\sigma_{bf}(p_\gamma/p_e)^2$; if the plasma is at some temperature T, then

$$\sigma_{\text{rec}} = \frac{2(\hbar\omega)^2}{c^2(m_e v)^2}\sigma_{bf} \cong 2\left(\frac{\epsilon_a}{m_e c^2}\right)\left(\frac{\epsilon_a}{k_B T}\right)\sigma_{bf} \simeq 10^{-22}\left(\frac{k_B T}{10 \text{ eV}}\right)^{-1} \text{cm}^2 \tag{1.49}$$

at the threshold with $\hbar\omega \simeq \epsilon_a \simeq 10$ eV. The rate of recombination per unit volume per second is $n^2 \sigma_{\text{rec}} v \equiv n^2 \alpha_R$, where $\alpha_R \simeq 2 \times 10^{-14}(k_B T/10 \text{ eV})^{-1/2}$ cm^3 s^{-1}.

In the analysis so far we have assumed that the recombination proceeds directly to the ground state. Such a process, however, will release a photon with energy $\hbar\omega \gtrsim \epsilon_a$ that will immediately ionise another atom. The net recombination actually proceeds through electron and proton, forming an excited state that decays to ground state later on. All the photons emitted in the process will have $\hbar\omega < \epsilon_a$ and cannot ionise the neutral atoms in the ground state. In this case, we can write a relation similar to relation (1.43) but with $\lambda = \lambda_1 = (2Zq^2/m_e v^2)$. Then the energy loss that is due to recombination is

$$\left(\frac{dE_{\text{rec}}}{dV dt}\right) \propto \left(\frac{1}{2} m_e v^2\right)(n_e n_i)\left[\frac{Zq^2}{(1/2) m_e v^2}\right]^2 v \propto n_e n_i v^{-1} \propto n^2 T^{-1/2}.$$

This can be one source of cooling for a plasma at $T \gtrsim 10^4$ K in addition to the bremsstrahlung cooling $(dE_{\text{bre}}/dV dt) \propto n^2 T^{1/2}$ obtained in Eq. (1.18). The net rate of cooling for a plasma can be expressed in the form $(dE/dV\,dt) = n^2\Lambda(T)$, where $\Lambda(T) = aT^{1/2} + bT^{-1/2}$; the first term which arises due to bremsstrahlung dominates for $T \gtrsim 10^6$ K.

When both photoionisation and recombinations occur in a region, the equilibrium is described by the relation $n_e n_i \alpha_R \simeq \sigma_{bf} n_H F$, where F is the flux of ionising photons with $\nu > \nu_I$. Taking $n_e = n_i = x n_0$, $n_H = (1 - x)n_0$, we can write this equation in the form

$$\frac{x^2}{(1-x)} \cong \left(\frac{\sigma_{bf}c}{\alpha_R}\right)\left(\frac{F}{n_0 c}\right) \simeq 5 \times 10^4 \left(\frac{T}{10^4\ \mathrm{K}}\right)^{1/2}\left(\frac{F}{n_0 c}\right), \tag{1.50}$$

which determines the ionisation fraction x in many astrophysical contexts. If a source of photons emitting $\dot{N}_\gamma$ ionising photons per second (with $\nu > \nu_I$) ionises a region of volume V around it, then the same argument gives $n_e^2 \alpha_R V \simeq \dot{N}_\gamma$. Taking $n_e = x n_0 \simeq n_0$, we get $V = (\dot{N}_\gamma / \alpha_R n_0^2)$.

It is also possible to imagine a situation in which the mean free path for collisions between atoms is small (so that the matter is in thermal equilibrium) but the mean free path for collisions between photons and matter is large (so that radiation is *not* in equilibrium with matter). In that case, the photons emitted by the system will escape from it with negligible scattering and there could arise radiation from atomic or molecular transitions, characteristic of composition. Then the amount of energy emitted per second by unit volume of gas, per unit frequency range, and solid angle can be written as

$$j_\nu = \left(\frac{dE}{d\Omega\, d\nu\, dt\, dV}\right) = \left[\frac{g_j}{Z}\exp\left(\frac{-h\nu_{ij}}{kT_s}\right)\right]\left(\frac{h\nu_{ij}}{4\pi}\right) Q_{ij} n \phi(\nu). \tag{1.51}$$

The first factor in the brackets gives the fraction of atoms in the excited state, with Z (the partition function) providing the normalisation. Because all the factors are known in this expression, it can be used to relate the source properties to the observed intensity. An important example of this is the 21-cm radiation from neutral hydrogen atoms. The intensity of this line and its width arising due to various effects, make it a useful probe of several systems.

1.5 Varieties of Astrophysical Structures

We now turn to the question of trying to determine broad features of astronomical systems from the description of the physical principles given above. It is clear, right at the outset, that we are interested in systems that are massive enough so that gravity plays a significant role in their dynamics. In the most extreme limit, we can think of the entire universe as a physical system and try to determine its structure. At sufficiently large scales, we can ignore the graininess in the distribution of matter and think of the universe as reasonably homogeneous and isotropic. Further, because no location in such a universe can be considered as special, any possible motion of matter on a large scale should also maintain the same characteristics with respect to any observer. It immediately follows that the most general motion consistent with these requirements must have the form $\mathbf{v}(t) = f(t)\mathbf{r}$, where $\mathbf{r}$ and $\mathbf{v}$ denote the position and the velocity, respectively, of any material body in the universe and $f(t)$ is an arbitrary function of time. This is the only kind of motion that is consistent with the requirement that from *any* point in the universe an observer will see matter moving in an identical manner. Using the fact that $\mathbf{v} = \dot{\mathbf{r}}$, this equation can be integrated to give $\mathbf{r} = a(t)\mathbf{x}$, where $a(t)$ is another arbitrary function related to $f(t)$ by $f(t) = (\dot{a}/a)$ and $\mathbf{x}$ is a constant for any given material body in the universe. It is conventional to call $\mathbf{x}$ and $\mathbf{r}$ the comoving and proper coordinates of the body and $a(t)$ the expansion factor (even though, if $\dot{a} < 0$, it acts as a contraction factor).

The dynamics of the universe is entirely determined by the function $a(t)$. The simplest choice will be $a(t) =$ constant, in which case there will be no motion in the universe and all matter will be distributed uniformly in a static configuration. It is, however, clear that such a configuration will be violently unstable when the mutual gravitational forces of the bodies are taken into account. Any such instability will eventually lead to random motion of particles in localised regions, thereby destroying the initial homogeneity. Observations, however, indicate that this is not true and that the relation $\mathbf{v} = (\dot{a}/a)\mathbf{r}$ does hold in the observed universe. In that case, the dynamics of $a(t)$ can be qualitatively understood along the following lines. Consider a particle of unit mass at the location $\mathbf{r}$, with respect to some coordinate system. Equating the sum of its kinetic energy $v^2/2$ and gravitational potential energy that is due to the attraction of matter within a sphere of radius r to a constant, we find that $a(t)$ should satisfy the condition

$$\frac{1}{2}\dot{a}^2 - \frac{4\pi G\rho(t)}{3}a^2 = \text{constant}, \tag{1.52}$$

where ρ is the mean density of the universe, that is,

$$\frac{\dot{a}^2}{a^2} + \frac{k}{a^2} = \frac{8\pi G}{3}\rho(t), \tag{1.53}$$

where k is a constant. Although the argument given above to determine this equation is fallacious, Eq. (1.53) happens to be exact and arises from the proper application of Einstein's theory of relativity to a homogeneous and isotropic distribution of matter. Observations suggest that our universe today (at $t = t_0$) is governed by this equation with $\rho(t_0) \approx 10^{-30}$ gm cm^{-3} and $(\dot{a}/a)_0 \equiv H_0 = 0.3 \times 10^{-17}h$ s^{-1}, where $h \approx 0.5$–1. This is equivalent to $H_0 = 100h$ km s^{-1} Mpc^{-1} where 1 Mpc $\approx 3 \times 10^{24}$ cm is a convenient unit for cosmological distances. (We will also use the units 1 kpc $= 10^{-3}$ Mpc and 1 pc $= 10^{-6}$ Mpc in our discussion.) From H_0 we can form the time scale $t_{\text{univ}} \equiv H_0^{-1} \approx 10^{10}h^{-1}$ yr and the length scale $cH_0^{-1} \approx 3000h^{-1}$ Mpc; t_{univ} characterises the evolutionary time scale of the universe and H_0^{-1} gives the largest length scales currently accessible in the universe.

The light emitted at an earlier epoch by an object will reach us today with the wavelengths stretched because of the expansion. If the light was emitted at $a = a_e$ and received today (when $a = a_0$), the wavelength will change by the factor $(1 + z_e) = (a_0/a_e)$, where z_e is called the redshift of the emitting object. The observed luminosity L of a source will decrease as $(1+z)^{-4}$, as L is proportional to $(p_\gamma c)\, d^3 p_\gamma \propto \nu^3 d\nu \propto (1+z)^{-4}$, where $p_\gamma = (\epsilon/c) = (h\nu/c)$ is the photon momentum.

If neither particles nor photons are created or destroyed during the expansion, then the number density of particles or photons will decrease as a^{-3} as a increases. In the case of photons, the wavelength will also get stretched during expansion with $\lambda \propto a$; because the energy density of material particles is nmc^2 whereas that of photons of frequency ν will be $nh\nu = (nhc/\lambda)$, it follows that the energy densities of matter and radiation vary as $\rho_{\rm rad} \propto a^{-4}$ and $\rho_{\rm matter} \propto a^{-3}$. Combining this result $\rho_{\rm rad} \propto a^{-4}$ with the result $\rho_{\rm rad} \propto T^4$ for thermal radiation, it follows that any thermal spectrum of photons in the universe will have its temperature varying as $T \propto a^{-1}$. In the past, when the universe was smaller, it would also have been (1) denser (2) hotter, and – at sufficiently early epochs – (3) dominated by radiation energy density. When the temperature of the universe was higher than the temperatures corresponding to the ionisation energy, the matter content in the universe was a high-temperature plasma.

Starting from such a hot initial plasma stage, the universe cools as it expands and eventually a variety of physical structures form in it. In the hot early phase, the radiation is in thermal equilibrium with matter; as the universe cools below $k_B T \simeq (\epsilon_a/10)$ the electrons and ions combine to form neutral atoms and radiation will decouple from matter. This occurs at $T_{\rm rec} \simeq 3 \times 10^3$ K, and the temperature of this radiation will continue to fall as $T \propto a^{-1}$. Observations show that the present universe is indeed bathed in such a thermal radiation field, with the current temperature being about $\sim$2.7 K. The energy density of this radiation today is $\rho_\gamma \simeq (k_B T)^4/(\hbar c)^3 \simeq 5.7 \times 10^{-13}$ erg cm^{-3}, which corresponds to a mass density of $(\rho_\gamma/c^2) = 5.7 \times 10^{-34}$ gm cm^{-3}. Taking the matter density today as $\rho_0 = 10^{-30}$ gm cm^{-3}, we find that $\rho_\gamma \simeq 5.7 \times 10^{-4} \rho_0$; radiation would have dominated over matter when the redshift was more than $z_{\rm eq} = 1.7 \times 10^3$. Also note that photons decoupled from matter when the universe was $(T_{\rm rec}/T_0) \simeq 10^3$ times smaller, i.e., at $z_{\rm rec} \simeq 10^3$.

These considerations were independent of the explicit form of $a(t)$. We now turn to the solutions of Eq. (1.53) that determine $a(t)$. The simplest solution to Eq. (1.53) will occur for $k = 0$ if we take the matter density in the universe as decreasing as a^{-3} with expansion. Then we get $a(t) = (t/t_0)^{2/3}$, where $t_0^{-2} = (6\pi G\rho_0)$ and $a(t)$ is normalised to $a = 1$ at the present epoch $t = t_0$. Such a totally uniform universe, of course, will never lead to any of the inhomogeneous structures seen today. However, if the universe had even the slightest inhomogeneity, then gravitational instability could amplify the density perturbations. To see how this comes about in the simplest context, consider Eq. (1.53) written in the equivalent form as

$$\ddot{a} = -\frac{4\pi G\rho_0}{3a^2} = -\left(\frac{2}{9t_0^2}\right)\frac{1}{a^2}, \tag{1.54}$$

where we have put $\rho = (\rho_0 a_0^3/a^3)$. If we perturb $a(t)$ slightly to $a(t) + \delta a(t)$ such that the corresponding fractional density perturbation is $\delta \equiv (\delta\rho/\rho) = -3(\delta a/a)$, we find that δa satisfies the equation

$$\frac{d^2}{dt^2}\delta a = \left(\frac{4}{9t_0^2}\right)\frac{\delta a}{a^3} = \frac{4}{9}\frac{\delta a}{t^2}. \tag{1.55}$$

This equation has the growing solution $\delta a \propto t^{4/3} \propto a^2$. Hence the density perturbation $\delta = -3(\delta a/a)$ grows as $\delta \propto a$. When the perturbations have grown sufficiently, their self-gravity will start dominating and the matter can collapse to form a gravitationally bound system. This can happen, for example, if the plasma in some local region can cool sufficiently fast. We now estimate the conditions for this.

1.5.1 $t_{\rm cool} \approx t_{\rm grav}$: Existence of Galaxies

The cooling of a plasma occurs mainly through two processes. The first is the radiation emitted during recombination of electrons and ions which, if it escapes the plasma, can be a source of recombination cooling. From the discussion in Subsection 1.4.4, we know that the recombination rate varies as $n^2T^{-1/2}$. The second is the bremsstrahlung cooling with an energy-loss rate proportional to $n^2T^{1/2}$ [see Eq. (1.18) with $n_i = n_e = n$]. For systems with temperature $k_BT \simeq (GMm_p/R)$, which is much higher than the ionisation potential, $\alpha^2 m_e c^2$, the dominant cooling mechanism is thermal bremsstrahlung. The cooling time for this process is

$$t_{\rm cool} \simeq \frac{nk_BT}{(d\mathcal{E}/dt\,dV)} = \left(\frac{\hbar}{m_ec^2}\right)\left(\frac{1}{n\lambda\!\!\!^{-}{}_e^3}\right)\left(\frac{k_BT}{m_ec^2}\right)^{1/2}\frac{1}{\alpha^3}, \tag{1.56}$$

and the time scale for gravitational collapse is

$$t_{\rm grav} \simeq \left(\frac{GM}{R^3}\right)^{-1/2}. \tag{1.57}$$

The condition for efficient cooling $t_{\rm cool} < t_{\rm grav}$, coupled with $k_BT \simeq GMm_p/R$, leads to the constraint $R < R_g$, where

$$R_g \simeq \alpha^3\alpha_G^{-1}\lambda\!\!\!^{-}{}_e\left(\frac{m_p}{m_e}\right)^{1/2} \simeq 74\ \text{kpc}, \tag{1.58}$$

where $\alpha_G \equiv (Gm_p^2/\hbar c) \approx 6 \times 10^{-39}$ is the gravitational (equivalent) of the fine-structure constant. In the above analysis we assume that $k_BT > \alpha^2 m_e c^2$; for

$R \simeq R_g$ this constraint is equivalent to the condition $M > M_g$, where

$$M_g \simeq \alpha_G^{-2}\alpha^5 m_p \left(\frac{m_p}{m_e}\right)^{1/2} \simeq 3 \times 10^{44} \text{ gm}. \tag{1.59}$$

This result suggests that systems having a mass of $\sim 3 \times 10^{44}$ gm and a radius of ~ 70 kpc could rapidly cool, fragment, and form gravitationally bound structures. Most galaxies have masses around this region. This is one possible scenario for forming galaxies. Note that the mass and the length scales in relations (1.59) and (1.58) arise entirely from the fundamental physical constants. We now consider some more properties of these structures.

The original (maximum) radius of the cooling plasma estimated above is ~ 70 kpc. After the matter has cooled and contracted, the final radius is more like 10–20 kpc, which is the typical radii of large galaxies. For $M_g \simeq 3 \times 10^{44}$ gm and $R_g \simeq 20$ kpc, the density is $\rho_{\rm gal} \simeq 10^{-25}$ gm cm^{-3}, which is $\sim 10^5$ times larger than the current mean density, $\rho_0 \simeq 10^{-30}$ gm cm^{-3}, of the universe. If we assume that high-density regions with $\bar{\rho} \gtrsim 100\bar{\rho}_{\rm univ}$ collapsed to form the galaxies, then the galaxy formation must have taken place when the density of the universe was ~ 1000 times larger; the value of $a(t)$ would have been 10 times smaller and the redshift of the galaxy formation should have been $z_{\rm gal} \lesssim 9$. If the protogalactic plasma condensations were almost touching each other at the time of formation, these centres (which would have been at a separation of ~ 150 kpc) would have now moved apart to a distance of $150(1 + z_{\rm gal})$ kpc ≈ 1500 kpc $= 1.5$ Mpc. This is indeed the mean separation between the large galaxies today. The nearest galaxy with a radius of ~ 10 kpc, at a distance of 1 Mpc, would subtend an angle of $\theta_{\rm gal} \approx 10^{-2}$ rad $\approx 30'$. A galaxy at a distance of ~ 4000 Mpc will subtend $0.5''$.

Observations have indicated that many different kinds of structures exist at redshifts of $z \lesssim 5$. Because the process of gravitational instability, which leads to the condensation of galaxy like objects, cannot be 100% efficient, it would leave some amount of matter uniformly distributed in between the galaxies. The light from distant galaxies will have to pass through this matter and will contain signature of the state of such an intergalactic medium (IGM). The photons (with $\nu > \nu_I$) produced in the first-generation objects could cause a significant amount of ionization of the IGM, especially the low-density regions. When a flux of photons (with $\nu > \nu_I$) impinge on a gas of neutral hydrogen with number density n_H, it will have an ionisation optical depth of $\tau = n_H \sigma_{bf} R$. Setting $\tau = 1$ gives a critical column density for ionisation to be $N_c \equiv n_H R = \sigma_{bf}^{-1} \simeq 10^{17}$ cm^{-2}. Regions with a hydrogen column density $N_c \simeq nR$ greater than 10^{17} cm^{-2} will appear as patches of neutral regions in the ionized plasma of the IGM. Such regions can be studied by absorption of light from more distant sources, (especially through Lyman alpha absorption corresponding to the transition between $n = 1$ and $n = 2$ levels) and are called Lyman alpha clouds.

Still larger structures than galaxies, called galaxy clusters, with masses of $\sim 10^{47}$ gm, a radius of ~ 3 Mpc, and a mean density of 10^{-27} gm cm^{-3}, exist in the universe as gravitationally bound systems. Our argument given above shows that the gas in these structures could not have yet cooled and will have a virial temperature of $T \approx (GMm_p/Rk_B) \approx 4 \times 10^7$ K.

Let us next investigate the nature of smaller-scale structures that can form inside a galaxy. Here, the existence of the different energy scales and equations of state allow for the possible existence of several – widely different – astrophysical systems, and most of these systems can be understood by systematic comparison of the energy scales $(\epsilon, \epsilon_a, \epsilon_{\rm nucl} \cdots)$ with ϵ_g.

1.5.2 $\epsilon_{\rm grav} \approx \epsilon_a$: Existence of Giant Planets

The laboratory systems have negligible gravitational potential energy; in a plot of (ϵ_F/k_BT) against (GMm_p/Rk_BT) they exist (almost) along the y axis [see Fig. 1.1 (top)]. We now see how gravity affects the structures as they get bigger. The atomic binding energy (per particle) of a system is approximately $\epsilon_a \approx \alpha^2 m_e c^2 \approx (q^2/a_0) \approx q^2 n^{1/3}$ if the atoms are closely packed (with $na_0^3 \simeq 1$), and the gravitational energy per particle is $\epsilon_g = (4\pi/3)^{1/3} G m_p^2 N^{2/3} n^{1/3}$. Their ratio is given by

$$\mathcal{R}_{ga} \equiv \frac{\epsilon_a}{\epsilon_g} \approx \left(\frac{\alpha}{\alpha_G}\right)\left(\frac{1}{N^{2/3}}\right) \equiv \left(\frac{N_G}{N}\right)^{2/3} \approx \left(\frac{10^{54}}{N}\right)^{2/3}. \qquad (1.60)$$

Clearly, the number $N_G \equiv \alpha^{3/2}\alpha_G^{-3/2} \approx 10^{54}$, arising out of fundamental constants, sets the smallest scale in astrophysics, in which the gravitational binding energy becomes as important as the electromagnetic binding energy of matter. The corresponding mass and length scales are $M_{\rm planet} \simeq N_G m_p \simeq 10^{30}$ gm and $R_{\rm planet} \simeq N_G^{1/3} a_0 \simeq 10^{10}$ cm and correspond to those of a large planet; for larger masses, gravitational interaction changes the structure significantly whereas for smaller masses gravity is ignorable and matter is homogeneous with constant density so that $M \propto R^3$.

Because we used Newtonian gravity to arrive at this conclusion, it is necessary to verify that the parameter $\mathcal{R}_{gm} \equiv (E_g/Mc^2)$ is small for this scale; this ratio for $M \simeq M_{\rm planet}$, $R \simeq R_{\rm planet}$ is $\mathcal{R}_{gm} = \alpha^2 (m_e/m_p) \ll 1$. Note that the smallness of $\mathcal{R}_{gm}$ follows purely from the values of fundamental constants.

Most of the astrophysically interesting systems have larger mass and require the gravitational force to be balanced by forces other than normal solid-state forces. In general, such systems can be classified into two categories. The first set has the gravitational force balanced by the kinetic energy of classical motion, whereas the second one has the gravitational force balanced by degeneracy pressure. For a system with $na_0^3 \approx 1$, the non-relativistic Fermi energy of electrons is comparable with the atomic binding energy and we can compare ϵ_a or ϵ_F with ϵ_g. This is meaningful as long as the temperature of the system is low

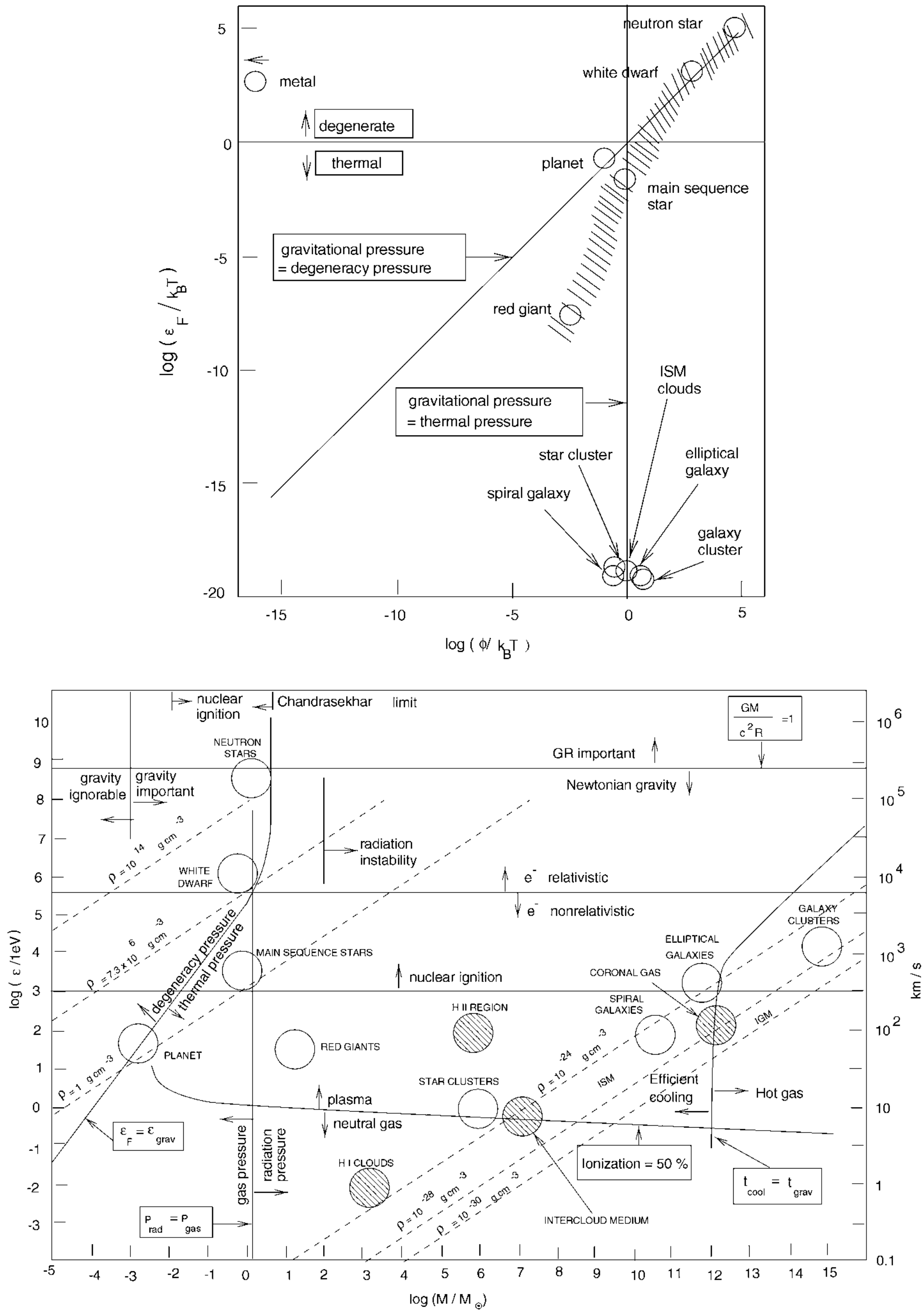

Fig. 1.1. Aspects governing the dynamics of various cosmic structures are summarised. See text for a detailed description.

and $k_B T \ll \epsilon_F \simeq \epsilon_a \approx 10$ eV. If the temperature is significantly higher, then it is the thermal energy $k_B T$ that should be compared with ϵ_g; that is, the gravitational pressure will be balanced by the Fermi pressure at low temperatures and by thermal pressure at high temperatures. We now examine such structures.

1.5.3 $\epsilon_{\rm grav} \simeq \epsilon_{\rm nucl}$*: Existence of Stars*

When the mass of the system is increased further, the gravitational pressure increases and – to balance it – both the Fermi pressure and the thermal pressure will increase. The dynamics of the system will then depend on the relative significance of these two quantities. To take into account both thermal and quantum degeneracy contributions, we take the matter pressure to be $P \approx nk_B T + n\epsilon_F$, which is a simple interpolation between the two limits. This pressure can balance the gravitational pressure if $(k_B T + \epsilon_F) \simeq Gm_p^2 N^{2/3} n^{1/3}$. Using expression (1.11) for ϵ_F for the non-relativistic electrons, we get

$$k_B T \simeq Gm_p^2 N^{2/3} n^{1/3} - \frac{(3\pi^2)^{2/3}}{2} \frac{\hbar^2}{m_e} n^{2/3}. \tag{1.61}$$

For a classical system, the first term on the right-hand side dominates, and we see that the gravitational potential energy and kinetic energy corresponding to the temperature T are comparable; this is merely a restatement of the virial theorem. As the radius R of the system is reduced, the second term on the right-hand side ($\propto n^{2/3}$) grows faster than the first ($\propto n^{1/3}$) and the temperature of the system will increase, reach a maximum, and decrease again; equilibrium is possible for any of these values with gravity balanced by thermal and degeneracy pressure. The maximum temperature $T_{\rm max}$ is reached when $n = n_c$, with

$$n_c^{1/3} \cong \frac{\alpha_G}{(3\pi^2)^{2/3}} \left(\frac{N^{2/3}}{\lambda\!\!\!^{-}_e} \right); \quad k_B T_{\rm max} \simeq \frac{\alpha_G^2}{2(3\pi^2)^{2/3}} (N^{4/3} m_e c^2), \tag{1.62}$$

where $\lambda\!\!\!^{-}_e \equiv (\hbar / m_e c)$ and $\alpha_G \equiv Gm_p^2 / \hbar c$.

An interesting phenomenon arises if the maximum temperature $T_{\rm max}$ is sufficiently high to trigger nuclear fusion in the system; then we obtain a gravitationally bound, self-sustained nuclear reactor. The condition for triggering nuclear reaction has to come from detailed study of the atomic nucleus and occurs typically at energy scales higher than $\epsilon_{\rm nucl} \approx \eta\alpha^2 m_p c^2$, with $\eta \simeq 0.1$. The energy corresponding to the maximum temperature $k_B T_{\rm max}$ will be larger than $\epsilon_{\rm nucl}$ when

$$N > (2\eta)^{3/4} (3\pi^2)^{1/2} \left(\frac{m_p}{m_e} \right)^{3/4} \left(\frac{\alpha}{\alpha_G} \right)^{3/2} \approx 4 \times 10^{56} \tag{1.63}$$

for $\eta \simeq 0.1$. The corresponding condition on mass is $M > M_*$, where

$$M_* \approx (2\eta)^{3/4} (3\pi^2)^{1/2} \left(\frac{m_p}{m_e} \right)^{3/4} \left(\frac{\alpha}{\alpha_G} \right)^{3/2} m_p \approx 4 \times 10^{32} \text{ gm}, \tag{1.64}$$

which is comparable with the mass of the smallest stars observed in our universe. The mass of the Sun, for example, is $M_\odot = 2 \times 10^{33}$ gm.

Comparison of relations (1.59) and (1.64) shows that the number of stars $N_* \simeq (M_g/M_*)$ in a typical galaxy will be given by the combination of fundamental constants $N_* = \alpha^{7/2}\alpha_G^{-1/2}(m_e/m_p)^{1/4} \simeq 10^{12}$. Typical galaxies indeed have approximately $10^{11} - 10^{12}$ stars, although there is a fair amount of spread in this number. The mean distance between stars in a galaxy will be $d_{\rm star} \approx (R_{\rm gal}/N_*^{1/3}) \approx$ 1 pc. A star like the Sun, with a radius of 10^{11} cm, located at a distance of 10 pc, will subtend an angle of about $\sim$1 milliarcsecond; it is clear that most stars will look like point objects.

1.5.4 Existence of H–R Diagram for Stars

Once the nuclear reactions occur at the hot central region of the gas cloud, its structure changes significantly. If the transport of this energy to the outer regions is through photon diffusion, then the opacity of matter will play a vital role in determining the stellar structure. In particular, the opacities determine the relation between the luminosity and the mass of the star.

A photon with mean free path $l = (n\sigma)^{-1}$, random walking through the plasma, will have $N_{\rm coll} \simeq (R/l)^2$ collisions in traversing the radius R. This will take the time $t_{\rm esc} \simeq (lN_{\rm coll}/c) \simeq (R/c)(R/l)$ for the photon to escape. The luminosity of a star L is the ratio between the radiant energy content of the star E_γ and $t_{\rm esc}$. Because $E_\gamma \simeq (aT^4)R^3$, where $a = (\pi^2 k_B^4/15\hbar^3 c^3) = (\pi^2/15) \simeq 1$ (in units with $k_B = \hbar = c = 1$), we find that $L = (aR^3T^4 l/R^2) \simeq RT^4 l$. For a wide class of stars, we may assume that the central temperature $T \simeq (GMm_p/R)$ is reasonably constant because nuclear reactions – which depend strongly on T – act as a thermostat. If Thomson scattering dominates, then $\sigma = \sigma_T$, and we get

$$L \simeq \frac{RT^4}{\sigma_T n} \simeq \frac{T^4 R^4}{\sigma_T N} \simeq \frac{G^4}{\alpha^2} m_p^5 m_e^2 M^3 \simeq 10^{34}\ \text{erg s}^{-1}\left(\frac{M}{M_*}\right)^3. \qquad (1.65)$$

If, on the other hand, the plasma is only partially ionised, we should use the opacities in expression (1.45), with $l \propto T^{7/2} n^{-2} \propto T^{7/2} R^6 M^{-2}$, and we have

$$L \propto RT^4 l \propto R^7 T^{15/2} M^{-2} \propto M^{11/2} R^{-1/2}.$$

Taking $R \propto M$ gives $L \propto M^5$. It is convenient to define the surface temperature T_s of the star by the relation $L \propto R^2 T_s^4$, so that $T_s \propto L^{1/4} R^{-1/2} \propto L^{1/4} M^{-1/2}$. Combining this result with the relation $M \propto L^{1/5}$, when the interior is only partially ionised, we get $T_s \propto L^{1/4} L^{-1/10} \propto L^{3/20}$. On the other hand, if Thomson scattering dominates with $L \propto M^3$, we get $T_s \propto L^{1/12}$. When the stars are plotted in a $\log T_s - \log L$ plane, (called the *H–R* diagram) we expect them to lie within the lines with slopes $(3/20) = 0.15$ and $(1/12) \simeq 0.08$. The observed slope is $\sim$0.13.

The temperature inside a star varies from approximately 10^8 K at the core to approximately a few thousand degrees Kelvin at the surface. The physical conditions, equation of state, and the opacity of matter vary significantly inside a star even when it is in a steady state. Further, when the stars evolve because of different nuclear processes, the response of matter to changing physical conditions can be dramatically different. We shall encounter many of these features in Volume II of this series.

The condensation of stars from galactic matter cannot also be a totally efficient phenomena, and we do expect a fair amount of matter to be distributed in the galaxy in different forms. This constitutes the interstellar medium (ISM) in which structures of very different densities and temperatures exist in pressure equilibrium. In our galaxy, the ISM contributes a mass of $\sim 10^9 M_\odot$ and has a pressure of approximately $P = nk_BT \simeq 10^{-12}$ dyn cm^{-2}. There exist a hot diffuse component ($T \simeq 10^6$ K, $n \simeq 10^{-3}$ cm^{-3}), a warm ionized component ($T \simeq 8000$ K, $n \simeq 10^{-1}$ cm^{-3}), a warm neutral component ($T \simeq 5000$ K, $n \simeq 10^{-1}$ cm^{-3}), a cold neutral component ($T \simeq 80$ K, $n \simeq 10$–100 cm^{-3}), and giant molecular clouds ($T \simeq 10$ K, $n \simeq 10^2$–10^5 cm^{-3}) in pressure equilibrium in the ISM. There are also processes that strongly couple the stars and the ISM. Consider, for example, the region around a hot star with $L = 3.5 \times 10^{36}$ erg s^{-1}, and $T_s \simeq 3 \times 10^4$ K. The number of ionizing photons $\dot{N}_\gamma$ (with $\nu > \nu_I$) emitted by such a star can be estimated from the Planck spectrum and will be approximately 3×10^{48} s^{-1}. In Subsection 1.4.4 we saw [see the discussion following relation (1.50)] that the volume of the region ionised by such a flux is given by $V = (\dot{N}_\gamma / \alpha n_0^2)$. Using $n_0 \simeq 10$ cm^{-3}, we find that matter will be fully ionised for a region of radius $R = (3V/4\pi)^{1/3} \simeq 10$ pc. At a distance of 5 pc from the star, relation (1.50) gives $(1 - x) \simeq 10^{-3}$, indicating nearly total ionisation. Such a local island of plasma in the ISM is called a HII region. The radiation from the plasma in HII region is one of the probes of the conditions of the ISM.

1.5.5 $\epsilon_{\rm grav} \simeq \epsilon_F$: Existence of Stellar Remnants

We saw above that stars are gravitationally bound systems in which self-sustaining nuclear reactions are taking place in the centre. For such systems, the kinetic energy and the potential energy are comparable and $Nk_BT \approx (GM^2/R)$. The process of combining four protons into a helium nuclei releases $\sim 0.03 m_pc^2$ of energy, which is $\sim 0.7\%$ of the original energy, $4m_pc^2$. Assuming that a fraction $\epsilon \approx 0.01$ of the rest-mass energy can be made available for nuclear reactions, we find that the lifetime of the nuclear burning phase of the star will be $t_{\rm star} = \epsilon M/L \approx 3 \times 10^9$ yr $(\epsilon/0.01)(M/M_*)^{-2}$ if the opacity is due to Thomson scattering. This defines the characteristic time scale in stellar evolution.

When the nuclear fuel in the star is exhausted, the gravitational force will start contracting the matter again and the density will increase. Eventually, the density will be sufficiently high so that the quantum degeneracy pressure will dominate over thermal pressure. The equilibrium condition for such a system will require the degeneracy pressure of matter to be large enough to balance gravitational pressure. Equivalently, the Fermi energy $\epsilon_F(n)$ must be larger than the gravitational potential energy $\epsilon_g \cong G m_p^2 N^{2/3} n^{1/3}$. When the particles are nonrelativistic, $\epsilon_F(n) = (\hbar^2/2m_e)(3\pi^2)^{2/3} n^{2/3}$ and the condition $\epsilon_F \geq \epsilon_g$ can be satisfied (at equality) if

$$n^{1/3} = \frac{2}{(3\pi^2)^{2/3}} \left(\frac{G m_p^2 m_e}{\hbar^2} \right) N^{2/3}. \tag{1.66}$$

With $n = (3N/4\pi R^3)$ and $N = (M/m_p)$, this reduces to the following mass–radius relation:

$$R M^{1/3} \simeq \alpha_G^{-1} \lambda\!\!\!^{-}_e m_p^{1/3} \simeq 8.7 \times 10^{-3}\, R_\odot M_\odot^{1/3}. \tag{1.67}$$

Such structures are called white dwarfs. A white dwarf with $M \simeq M_\odot$ will have $R \simeq 10^{-2} R_\odot$ and density $\rho \simeq 10^6 \rho_\odot$.

As the density increases, electrons combine with protons through inverse beta decay to form neutrons, which can provide the degeneracy pressure. Equation (1.66) is still applicable with m_e replaced with m_n; correspondingly the right-hand side of relation (1.67) is reduced by $(\lambda\!\!\!^{-}_n/\lambda\!\!\!^{-}_e) = (m_e/m_n) \simeq 10^{-3}$. Such objects – called neutron stars – will have a radius of $R \simeq 10^{-5} R_\odot$ and a density of $\rho \simeq 10^{15} \rho_\odot$ if $M \simeq M_\odot$. For such values $\mathcal{R}_{gm} \simeq 1$ and general relativistic effects are beginning to be important.

When the density is still higher, the Fermi energy has to be supplied by relativistic particles, and ϵ_F now becomes $\epsilon_F \simeq \hbar c n^{1/3}$, which scales as $\epsilon_F \propto n^{1/3}$, just like ϵ_g. Therefore the condition $\epsilon_F \geq \epsilon_g$ can be satisfied only if $\hbar c \geq G m_p^2 N^{2/3}$ or $N \leq \alpha_G^{-3/2} \simeq N_G \alpha^{-3/2}$. The corresponding mass bound (called Chandrasekhar limit) is $M \lesssim m_p \alpha_G^{-3/2} \simeq 1 M_\odot$. (A more precise calculation gives a slightly higher value.)

If the mass of the stellar remnant is higher than $\alpha_G^{-3/2} m_p$, no physical process can provide support against the gravitational collapse. In such a case, the star will form a black hole and is likely to exert a very strong gravitational influence on its surroundings. More complicated processes can lead to the formation of black holes with masses significantly higher than stellar masses in the centres of galaxies. Whenever such a localised centre of a high gravitational field is formed in the form of neutron stars or black holes, a wide variety of new physical phenomena can take place in that vicinity, essentially involving accretion of matter. In an accretion process, the gravitational potential energy is converted into the kinetic energy of matter and dissipated as thermal radiation. Some of the very high-energy sources of radiation – both galactic and extra galactic – are generally believed to be powered by such an accretion process. On the galactic scale, accretion discs around stars can be a source of thermalised x-ray emission;

in the extragalactic domain there are objects called active galactic nuclei and quasars that have a luminosity of $\sim 10^{44}$ erg s^{-1}, which are thought to be powered by accretion discs around very massive black holes.

The dynamical aspects of different structures in the universe discussed so far are summarised in Fig. 1.1. In the top part of the figure, various cosmic structures are classified by two ratios: $(\epsilon_F/k_B T)$ and $(GMm_p/Rk_B T)$. Objects with negligible self-gravity lie along the y axis (with $x \simeq 0$); a simple example of this is small-scale matter in the laboratory, like a piece of a metallic solid with the size of a few cubic meters, say. (Such a metal actually goes out of scale in the figure and is shown on the top left with an arrow indicating the fact that it is out of scale.) The line $x = 1$ corresponds to $k_B T = (GMm_p/R)$, implying that in these structures gravity is supported by thermal pressure. Among such objects, those with negligible Fermi energy will lie in the lower part of the figure. It can be seen that star clusters, clouds in the ISM, spiral and elliptical galaxies, clusters of galaxies, etc., all lie around the line $x = 1$ in the lower half of the diagram. For these systems, we have interpreted the mean kinetic energy as providing an equivalent temperature, when necessary. The line $y = 1$ corresponds to $\epsilon_F = k_B T$ so that the upper part of the diagram corresponds to systems dominated by degeneracy effects ($\epsilon_F > k_B T$) and the lower part is dominated by thermal effects ($\epsilon_F < k_B T$). We note that objects such as neutron stars and white dwarfs are dominated by degeneracy effects whereas the rest of astrophysical structures can be interpreted in classical terms. Finally, the line $x = y$ corresponds to $\epsilon_F = (GMm_p/R)$ and represents structures in which gravity is supported by degeneracy pressure. They lie along in the upper right half of the figure.

The bottom part of the figure describes these structures from a different and more detailed perspective. The y axis is the the dominant internal energy per particle, and the x axis denotes the mass of different structures. For unfilled circles (planets, main-sequence star, red giants, white dwarfs, neutron stars, star clusters, spiral and elliptical galaxies, and clusters of galaxies) the internal energy is gravitational potential energy per particle. The filled circles denote the components in the ISM (molecular clouds, intercloud medium and hot ionised gas, HII regions) and for these objects the internal energy is taken to be the thermal energy. In the latter case the density n and the temperature T are used to obtain an effective mass and radius by means of the relations $M = (4\pi/3)m_p n R^3$, $GMm_p/R = k_B T$. The equivalent velocity corresponding to the internal energy is shown on the y axis along the right-hand side; it is computed by the relation $\epsilon = (1/2)m_p v^2$.

The nearly horizontal line around 1 eV separates ionised hydrogen gas from neutral with the line corresponding to 50% ionization. The other three horizontal lines around 1 keV, 1 MeV, and 1 GeV demarcate energy scales corresponding to nuclear ignition, pair production of e^+e^-, and the black-hole limit. Assuming that the internal energy ϵ is comparable with gravitational self-energy

GMm_p/R, we can determine the scalings for the radius $R \propto M/\epsilon$ and density $\rho \propto M/R^3 \propto \epsilon^3/M^2$; the lines of constant ρ are given by $\epsilon \propto M^{2/3}$, which are marked for different values of density by dashed lines.

The unbroken curve on the left is obtained when Fermi energy is equated to gravitational energy and corresponds to the $x = y$ line in the upper part of the figure. We see that neutron stars, white dwarfs, and even large planets lie along this line and also that neutron stars are close to the $GM/c^2R = 1$ line, which decides whether general relativistic effects are important. For the planet, the Fermi energy is comparable with the atomic binding energy and gravity is just marginally important; this fact is indicated by a small vertical line near the left top. The main-sequence stars lie away from the degeneracy line and are essentially thermally supported; they are also, of course, above the line for nuclear ignition.

To the right-hand side of the figure we have a bending, unbroken curve that we obtain by equating the cooling time scale for plasma to the gravitational collapse time scale. Material to the left of this curve cool efficiently and we find that spiral and elliptical galaxies lie on this side; the galaxy clusters, on the other hand, lie to the right and will contain hot plasma.

In between the two extremes, some of the components of the ISM and the IGM have been marked. The molecular clouds, intercloud medium, and the coronal gas are actually in pressure equilibrium and lie along a line corresponding to $p \propto nT =$ constant. (Because, for these objects, $M \propto nR^3$ and $\epsilon \propto T \propto M/R$, it follows that $p \propto nT \propto \epsilon^4/M^2$. Lines of constant p correspond to $\epsilon \propto M^{1/2}$.)

Much of the discussion in the preceding sections is summarized in this Fig. 1.1 and Table 1.1, which also shows the large dynamic range spanned by the astrophysical systems, with, for example, the density varying from 10^{-30} g cm^{-3} in the IGM to 10^{15} g cm^{-3} in the neutron star.

1.6 Detecting the Photons

The universe has been studied in a wide variety of wave bands from very long waves ($\simeq$10 m) to ultrahigh-frequency γ-ray bands. We now summarize the main sources in various wave bands.

1.6.1 Role of Earth's Atmosphere

To begin with, it must be noted that the energy levels of atoms and molecules have an important implication for observational astronomy. Ground-based observations can detect only radiation that can penetrate through the Earth's atmosphere. The atoms of most elements have energy levels of the order of $E_0 \approx (1/2)\alpha^2 m_e c^2 \approx 10$ eV. Using the relation between photon energy and wavelength, $(E/1 \text{ eV}) \approx (\lambda/12345)^{-1}$ Å, we conclude that photons with $\lambda \lesssim 10^3$ Å will be absorbed by the atmosphere, leading to ionisation of the upper layers.

Table 1.1. Structures in the universe

Object	Mass (gm)	Radius (cm)	$\sigma = (GM/R)^{1/2}$ (km s^{-1})	$\rho = 3M/4\pi R^3$ (gm cm^{-3})
Jupiter	2×10^{30}	6×10^9	47	2.3
Sun	2×10^{33}	7×10^{10}	470	1.4
Red giant	$(2\text{–}6) \times 10^{34}$	10^{14}	37–63	$(4.8\text{–}14.3) \times 10^{-9}$
White dwarf	2×10^{33}	10^8	3×10^4	5×10^8
Neutron star	3×10^{33}	10^6	1.4×10^5	7×10^{14}
Global cluster	1.2×10^{39}	1.5×10^{20}	8.4	8.5×10^{-23}
Open cluster	5×10^{35}	3×10^{19}	0.3	4.4×10^{-24}
Spiral	$2 \times (10^{44}\text{–}10^{45})$	$(6\text{–}15) \times 10^{22}$	150–300	$(14\text{–}22) \times 10^{-26}$
Elliptical	$2 \times (10^{43}\text{–}10^{45})$	$(1.5\text{–}3) \times 10^{23}$	30–210	$(0.14\text{–}1.8) \times 10^{-26}$
Group	4×10^{46}	3×10^{24}	300	3.5×10^{-28}
Cluster	2×10^{48}	1.2×10^{25}	10^3	2.7×10^{-28}
Universe	$7.5 \times 10^{55}\Omega h^{-1}$	$10^{28}h^{-1}$	$2.2 \times 10^5\Omega^{1/2}$	$1.8 \times 10^{-29}\Omega h^2$

Further, the rotational- and the vibrational-energy levels of molecules such as H_2O and CO_2 (which exist in the atmosphere) fall within the IR band; this causes the IR radiation also to be absorbed by the atmosphere, although to somewhat lesser degree than the higher energy radiation. Because of these effects, the ground-based observations are essentially limited to visible ($\lambda \approx 3000$–6000 Å, $\nu \approx 10^{15}$–5×10^{14} Hz) and radio ($\lambda > 1$ cm, $\nu < 3 \times 10^{10}$ Hz) waves.

There is, however, another limitation arising from the fact that very long wavelength radiation ($\lambda \gtrsim 100$ m) cannot propagate through the plasma in the ionosphere and is reflected back. Consider an electromagnetic wave that moves the electrons in a plasma (relative to ions) by a small distance δx along the x axis. This deposits a charge $Q \simeq e(nA\delta x)$ on a fictitious surface of area A perpendicular to the x axis. This charge density, in turn, will lead to an electric field $E_x \simeq 4\pi(Q/A) \simeq 4\pi en\delta x$ that acts on the electrons in this small volume, pulling them back. Such a restoring force, proportional to displacement, gives electrons a characteristic frequency of oscillation (called plasma frequency):

$$\omega_p = \left(\frac{4\pi e^2 n}{m}\right)^{1/2} = 5.64 \times 10^4 \text{ Hz}\left(\frac{n}{1 \text{ cm}^{-3}}\right)^{1/2}. \tag{1.68}$$

Waves with frequencies lower than the plasma frequency cannot propagate through a plasma as the electrons can redistribute themselves sufficiently quickly to cancel the field of such an electromagnetic wave. We can estimate the number density n of electrons in the ionosphere by equating the ionisation rate that is due to solar radiation with the recombination rate, as done above for HII regions. This gives an electron density of approximately 4×10^5 cm^{-3}; the corresponding plasma frequency is approximately $\nu_p = (\omega_p/2\pi) = 6$ MHz. Thus we cannot observe radio waves with frequencies lower than ~6 MHz, corresponding to wavelengths larger than about ~50 m. To obtain information about all other wavelength regimes, it is necessary to make observations at high altitudes: from balloons, aircrafts, spacecrafts, satellites, etc. We now consider each band separately.

1.6.2 Radio

$$(\lambda = 3\,\text{cm–}10\,\text{m}, \quad \nu \simeq 3 \times 10^7\text{–}10^{10}\ \text{Hz}, \quad T \simeq 10^{-3}\text{–}0.5\ \text{K}).$$

Several discrete sources (supernova remnants, radio galaxies, quasars, etc.) emit radio waves essentially because of synchrotron process. As a specific example, consider the diffuse radio background in our galaxy that is due to synchrotron radiation from electrons in the ISM. Observations indicate that the spectrum of the electrons is given by $(dN/dE) \simeq 3 \times 10^{-11} E^{-3.3}$ particles cm^{-3}, if E is measured in giga–electron-volts. If the magnetic field is approximately 6×10^{-6} G, the relation (1.22) will predict a volume emissivity of

$$j_\nu \simeq 3 \times 10^{-38} \left(\frac{\nu}{10\ \text{MHz}} \right)^{-1.1} \text{erg s}^{-1}\ \text{cm}^{-3}\ \text{Hz}^{-1}. \tag{1.69}$$

This is close to the observed background emission. Over a line of sight of 1 kpc, this will give a flux of 10^{-20} W m^{-2} rad^{-2} Hz^{-1}. Similar power-law radio spectra are seen in the case of radio galaxies, quasars, etc., and are thought to be due to synchrotron radiation.

Along the spiral arms of galaxies, there exist clouds of HII regions that emit thermal bremsstrahlung radiation with a relatively flat spectrum. For example, the HII regions in Orion have $T \simeq 10^4$ K, $n_i \simeq 2 \times 10^3$ cm^{-3}, and an effective line-of-sight thickness of 6×10^{-4} pc. From Eq. (1.17) we can estimate the flux to be approximately 3×10^{-21} erg m^{-2} s^{-1} Hz^{-1} rad^{-2} = 300 Jansky, where 1 Jansky $\equiv$ 1 Jy = 10^{-26} W m^{-2} sr^{-1} Hz^{-1}. This is typical of emission from HII regions. The total diffuse radio emission from the galaxy is in the range 10^{29}–10^{33} W.

Radio galaxies are another main class of radiators in this band with a complicated pattern of emission. The radiation usually arises from two blobs on either side of the central galaxy with a separation ranging from 3 kpc to 1 Mpc. The power from these radio sources is quite high: 10^{33}–10^{39} W; special models are needed to explain this emission. The flux that is due to such a source at a distance of 3000 Mpc will be approximately 10^{-16} W m^{-2} sr^{-1}.

Radio observations can also detect the presence of neutral hydrogen in the universe through the 21-cm radiation discussed in Subsections 1.4.1 and 1.4.2. Because $h\nu \ll k_B T$ in most cases involving 21-cm radiation, g/Z in Eq. (1.51) is essentially the ratio of spin states $g_1/(g_1 + g_0)$, which is 3/4 for the hydrogen hyperfine transition. The total intensity from an optically thin column of length L will be (for $h\nu \ll k_B T$)

$$I_\nu \cong j_\nu L \cong \frac{3}{16\pi}\left(\frac{hc}{\lambda}\right) Q_{21\mathrm{cm}}(nL)\phi_\nu. \tag{1.70}$$

The corresponding brightness temperature $T_B(\nu) \equiv (\lambda^2 I_\nu/2k_B)$ is given by

$$T_B(\nu) = \frac{3}{32\pi}\left(\frac{hc\lambda}{k_B}\right) Q_{21} N\phi(\nu), \tag{1.71}$$

where N is the column density of the hydrogen along the line of sight. The observed form of $T_B(\nu)$ will contain information about N as well as the features of the source (such as its motion) that lead to the broadening of the line.

Neutral hydrogen at a redshift of z can be detected by observations at the wavelength of $21(1+z)$ cm, which is in the radio band for sources with the redshift in the range of, say, $z \simeq 0$–10.

The faintest detectable flux in this band is $\sim$1 mJy; there are $\sim 10^6$ discrete sources in the sky up to this level. The diffuse background in the radio band arises from our galactic disk, halo, and unresolved extragalactic radio sources. The background flux varies from approximately 3×10^4 Jy at 100 cm to 6×10^5 Jy at 10^4 cm.

1.6.3 Microwave and Submillimeter

$$(\lambda = 0.02\text{–}3\ \text{cm}, \quad \nu \simeq 10^{10}\text{–}3 \times 10^{12}\ \text{Hz}, \quad T = 0.5\text{–}300\ K)$$

The discrete sources in this band are usually dust clouds, hydrogen gas, and quasars. The background radiation in this band, however, is of tremendous theoretical importance and has been studied extensively. (In fact, this band has the maximum intensity of background radiation.) It turns out that the major component of the background radiation in the microwave band can be fitted very accurately by a thermal spectrum at a temperature of about $\sim$2.7 K. It seems reasonable to interpret this radiation as a relic arising from the early, hot phase of the evolving universe. The νB_ν for this radiation peaks at a wavelength of 1 mm and has a maximum intensity of 5.3×10^{-7} W m^{-2} rad^{-2} over the entire sky. The intensity per square arcsecond of the sky is approximately 1.33×10^{-17} W m^{-2} arc sec^{-2}.

Microwave radiation is also a sensitive probe of the structure-formation scenario along the following lines: The gravitational potential that is due to a density perturbation $\delta\rho = \bar{\rho}\delta$ in a region of size R will be $\phi \propto \bar{\rho}\delta R^2$. In an expanding universe $\bar{\rho} \propto a^{-3}$ and $R \propto a$ and the perturbation δ grows as $\delta \propto a$ [see discussion following Eq. (1.55)], making ϕ constant in time. Because photons climbing out of a potential well of size ϕ will lose energy and undergo a redshift

$(\Delta\nu/\nu) \approx (\phi/c^2)$, we would expect to see a temperature anisotropy in the microwave radiation of the order of $(\Delta T/T) \approx (\Delta\nu/\nu) \approx (\phi/c^2)$. The largest potential wells would have left their imprint on the cosmic background radiation at the time of decoupling of radiation and matter. The galaxy clusters constitute the deepest gravitational potential wells in the universe from which the escape velocities are $v_{\rm clus} \approx (GM/R)^{1/2} \approx 10^3$ km s^{-1}. This will lead to a temperature anisotropy of $\Delta T/T \approx (v_{\rm clus}/c)^2 = 10^{-5}$. Such a temperature perturbation has indeed been observed in microwave background radiation, vindicating the ideas for structure formation.

1.6.4 Infrared

$$(\lambda \simeq 8000\ \text{Å}–0.01\ \text{cm}, \quad \nu \simeq 3 \times 10^{12}–10^{14}\ \text{Hz}, \quad T = 300–4000\ \text{K})$$

Several interesting astrophysical processes contribute in this band, the most prominent being dust, which, when irradiated by some luminous source and heated to the temperature range of 400–4000 K emits IR. However, this is one of the most difficult ranges of frequencies to study owing to the enormous opacity of Earth's atmosphere as well as contamination that is due to emission from interstellar and interplanetary dust. In addition, hydrogen and dust clouds in our galaxy and outside galaxies as well as star-forming regions in our galaxy contribute to this band. The near-IR band of $(1–10) \times 10^{-4}$ cm will also receive contributions from the redshifted light associated with the initial epoch of galaxy formation. There have been several attempts to subtract out the galactic contamination and obtain the extragalactic *IR* flux. Although firm upper bounds are available, there is still substantial uncertainty about the actual shape of the background *IR* spectrum. The faintest detectable flux is $\sim$1.0 Jy and there are about $\sim 10^4$ discrete sources up to this limit.

1.6.5 Optical and Ultraviolet

$$(\lambda \simeq 100–8000\ \text{Å}, \quad \nu \simeq 8 \times 10^{14}–3 \times 10^{16}\ \text{Hz}, \quad T = (4000–3 \times 10^4\ \text{K})$$

This range of wavelengths includes visible, UV, far UV, and even what may be called soft x-ray. Most of the astronomical observations are still carried out in the optical band, in which we can reach up to 10^{-6} Jy. Stars, galaxies, and quasars contribute dominantly in this band; there are $\sim 10^{10}$ discrete sources in the sky. This spectral region also gets a large amount of line radiation from atomic gaseous systems.

Given the luminosity L and the radius R of a star, its effective surface temperature is determined by the equation $L = (4\pi R^2)(\sigma T_{\rm eff}^4)$. For the Sun, this gives $T_{\rm eff} \approx 5500$ K; the Planckian radiation corresponding to this temperature will peak around $\lambda \approx 5500$ Å (in the visible band). The flux of radiation from such a star located at a distance of 10 pc will be approximately $F = 3 \times 10^{-10}$ W m^{-2}. It is conventional in astronomy to use a unit called the bolometric magnitude, m, to indicate the flux where F and m are related approximately by $\log F \cong -8\text{–}0.4(m-1)$ when F is measured in Watts per square meter. When the flux changes by 1 order of magnitude, the magnitude changes by 2.5. A sunlike star at 10 pc will have a magnitude of $\sim$4.6.

Starlight also contributes to the sky background in the optical band. A solid angle $d\Omega$ will intercept a volume $(1/3)R^3 d\Omega$ of our galaxy if R is the radius of the galaxy. If the number density of bright stars with luminosity $L_\odot$ is $n(\simeq 0.1\ \text{pc}^{-3})$, then the flux per steradian is $[(1/3)nR^3 L_\odot / 4\pi(R/2)^2] \simeq (1/3\pi)nL_\odot R \simeq 2.4 \times 10^{-5}$ W m^{-2} rad^{-2} if $R = 10$ kpc. Using 1 rad$^2 \simeq 4 \times 10^{10}$ arc sec^2, we get a sky brightness that is due to integrated starlight of approximately 6×10^{-16} W m^2 arc sec^{-2}. In other words, the sky background that is due to integrated starlight provides $\sim$21 mag arc sec^{-2}.

We have seen above that a galaxy consists of $\sim 10^{11}$ stars and could be located at distances ranging from 1 to 4000 Mpc. At 10 Mpc, such a galaxy will subtend an angle of approximately $\theta \simeq (2R/d) \simeq 200''$ and will have a flux of approximately 3×10^{-11} W m^{-2} if the size of the galaxy $R_{\text{gal}} \simeq 10$ kpc. The surface brightness of the galaxy will be $\sim 10^{-16}$ W m^{-2} arc sec^{-2} or, equivalently, $\sim$21 mag arc sec^{-2}. These galaxies also contribute to the background light in the optical band. Repeating the above analysis we did for stars with $L = 10^{11} L_\odot$, $R \simeq 4000$ Mpc, and $n \simeq 1$ Mpc^{-3}, we get a background of 2×10^{-17} W m^{-2} arc sec^{-2}, equivalent to 24.5 mag arc sec^{-2}.

We still do not have conclusive evidence that suggests the existence of a smooth background in this band. As there is a large amount of contamination from zodiacal light, backscattering of radiation from interstellar gas, and hot stars in the field of view, these observations are quite difficult.

1.6.6 *X Ray and γ Ray*

$$(\lambda = 3 \times 10^{-3}\text{–}100\ \text{Å}, \quad \epsilon \simeq 0.12\text{–}400\ \text{keV}, \quad T = 3 \times 10^4\text{–}10^9\ \text{K})$$

Because x rays and γ rays are strongly absorbed in the Earth's atmosphere, observations in this wave band need to be carried out from outside the atmosphere from x-ray satellites. Equivalent temperatures of $\sim 10^8$ K are required for producing hard x-rays. Besides in the central cores of stars, such high energies can be usually found only in binary stars and in supernova remnants. The accretion of matter from one star to a compact companion can lead to the production of x-rays; so can the explosion of a supernova.

The process of accretion works along the following lines. When a mass m falls from infinite distance to a radius R, in the gravitational field of a massive object with mass M, it gains the kinetic energy $E \simeq (GMm/R)$. If this kinetic energy is converted into radiation with efficiency ϵ, then the luminosity of the accreting system will be $L = \epsilon(dE/dt) = \epsilon(GM/R)(dm/dt)$. The photons that are emitted by this process will be continuously interacting with the in-falling particles and will be exerting a force on the ionised gas. When this force is comparable with the gravitational force attracting the gas towards the central object, the accretion will effectively stop. The number density $n(r)$ of photons crossing a sphere of radius r, centred at the accreting object of luminosity L, is $(L/4\pi r^2)(\hbar\omega)^{-1}$, where ω is some average frequency. The rate of collisions between photons and the electrons in the ionised matter will be $[n(r)\sigma_T]$ and each collision will transfer a momentum $(\hbar\omega/c)$. Because electrons and ions are strongly coupled in a plasma, this force will be transferred to the protons. Hence the outward force on an in-falling proton at a distance r will be

$$f_{\text{rad}} \simeq (n\sigma_T)\left(\frac{\hbar\omega}{c}\right) = \left(\frac{L}{4\pi r^2}\right)\left(\frac{1}{\hbar\omega}\right)\sigma_T\left(\frac{\hbar\omega}{c}\right) = \left(\frac{L\sigma_T}{4\pi c r^2}\right). \quad (1.72)$$

This force will exceed the gravitational force attracting the proton, $f_g = (GMm_p/r^2)$, if $L > L_E$, where

$$L_E = \frac{4\pi G m_p c}{\sigma_T} M \simeq 1.3 \times 10^{46}\left(\frac{M}{10^8 M_\odot}\right) \text{erg s}^{-1} \quad (1.73)$$

is called the Eddington luminosity. The temperature of a system of size R radiating at L_E will be determined by $(4\pi R^2)\sigma T^4 = L_E$, that is,

$$T \simeq 1.8 \times 10^8 \text{ K}\left(\frac{M}{M_\odot}\right)^{1/4}\left(\frac{R}{1 \text{ km}}\right)^{-1/2}. \quad (1.74)$$

For a solar-mass compact ($R \simeq 1$ km) star this radiation will peak in the x-ray band.

The main extragalactic sources of x-rays are quasars and hot ionised gas in clusters of galaxies. Taking the cluster gas to be fully ionized hydrogen with a mass of approximately $M_{\text{gas}} = 10^{48}$ gm spread over a sphere of radius $R \simeq 3$ Mpc, we can estimate the number density of ions and electrons as $n_e \approx (M_{\text{gas}}/m_p V) \approx 10^{-4}$ cm^{-3}, where V is the volume of the cluster. Such a gas will be a source of thermal bremsstrahlung radiation at the rate of $L = 1.42 \times 10^{-27}\, n_e^2 T^{1/2}$ erg s^{-1} cm^{-3} [see Eq. (1.18)] where all quantities are in cgs units. Using the estimated values of n_e and T, we get the total luminosity from the whole cluster to be $\mathcal{L} = LV \approx 5 \times 10^{44}$ erg s^{-1}. This radiation will be in the wave band corresponding to the temperature of 10^8 K, which is in x-rays. Several such x-ray–emitting clusters have been observed.

In addition, there exists a well-defined diffuse x-ray background in the range of 1 keV to 100 MeV. Part of this background could be due to unresolved pointlike sources and another part may be due to hot ($T \simeq 10^9$ K) diffuse, intergalactic plasma. In the range 3–50 keV it can be fitted by an optically thin thermal bremsstrahlung at the temperature 40 ± 5 keV.

No object in the universe is hot enough to produce high-energy γ rays by thermal radiation. The γ rays are produced by accretion of matter on compact objects and by the collision of high-energy particles in the cosmic rays with the nuclei of atoms in our galaxy.

Figure 1.2 summarizes the electromagnetic spectra of the universe. In the top part of the figure the y axis is the flux per logarithmic band, $F \equiv \nu F_\nu$ in units of watts per square meter. The corresponding bolometric magnitude m, related to flux by $\log F = -8\text{–}0.4(m-1)$, is shown along the y axis on the right. The

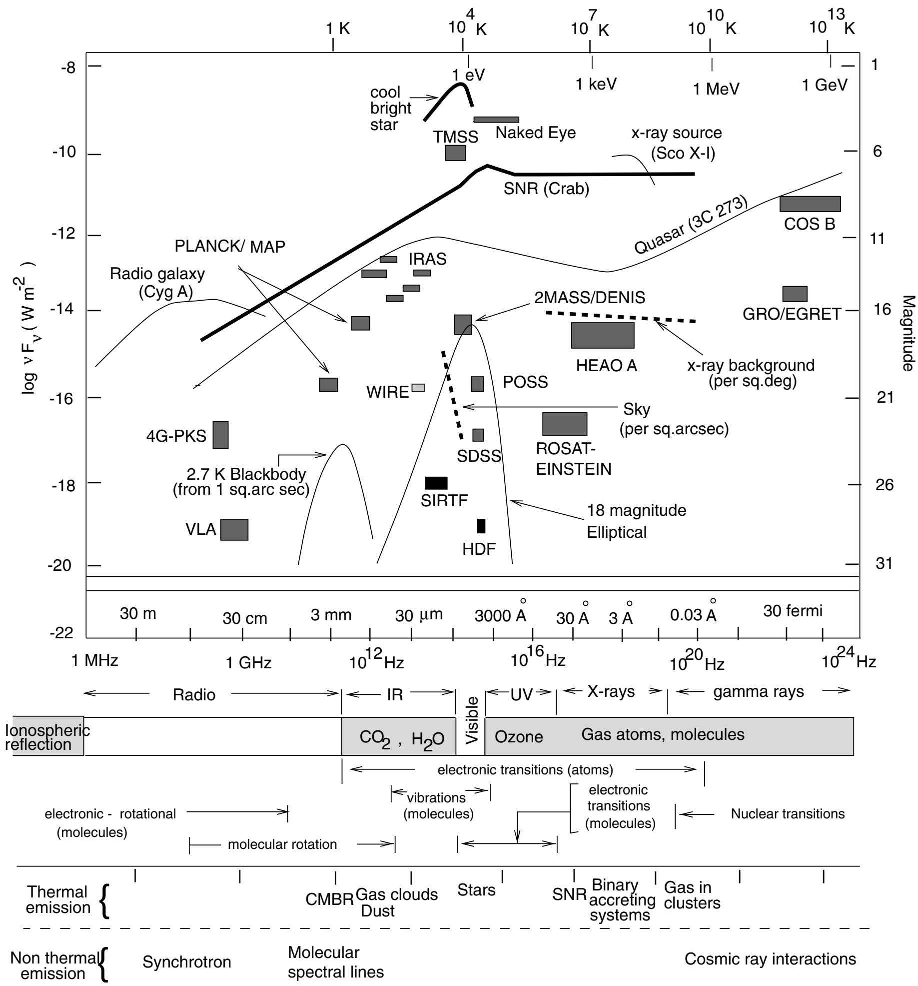

Fig. 1.2. This figure summarises the variety of radiative phenomena in astrophysics. The top part of the figure gives the spectra of a class of objects and the effective sensitivities reached in the surveys in different wave bands. The bottom part gives (1) the atmospheric absorption, (2) the key processes contributing to line radiation, (3) major thermal sources, and (4) main sources of nonthermal emission in different spectral bands.

main x axis is marked in both frequency and wavelength at the bottom and in equivalent temperature, obtained by $k_B T = h\nu$, along the top. The bottom part of the figure gives several general features discussed above. The first panel below the x axis divides the frequency range into different wave bands and indicates the major components of the atmosphere that absorb the radiation in each band. The next panels indicates the processes which can lead to line emission in each of the wave bands. Finally, the main sources of thermal and nonthermal radiation in different wavebands are summarized in the last two panels.

In the main figure, the typical spectra from different sources as well as the detection limit of different instruments in various bands are shown. A bright star, close to $m = 1$ and peaked in optical, has the maximum flux. Other sources are (1) a typical supernova remnant marked SNR (Crab), (2) a radio galaxy Cygnus-A, (3) a quasar (3C273) with emission in several wave bands, (4) an 18th-magnitude elliptical galaxy, and (5) a bright–x-ray source Sco X-1. In addition to these sources, also marked are (1) the flux from the cosmic microwave background radiation from one square arc second of the sky, (2) x-ray background per square degree that is due to unresolved sources, and (3) the sky background per square arc second in the optical band. The filled rectangular boxes are the detection limits of different probes operating in various bands. Many of these, like IRAS, HEAO, ROSAT-Einstein, GRO-EGRET, COS-B, and of course, the Hubble space telescope, are satellite-based instruments. Some of the points marked in the optical band like the Hubble deep field (HDF), come from integrated–pencil-beam kind of surveys, whereas many other limits are applicable to wider-band surveys. This figure summarizes our current technological capabilities as well as the expected flux in different astrophysical contexts.

Exercise 1.1

Why the rest of the book? Arguments similar to the ones given in this chapter are appealing as they *seem* to capture the essence of the physics behind each of the phenomena. Investigate carefully whether this is indeed true. In particular, ask (1) Are the scaling relations obtained by such arguments trustworthy? (2) Are the numerical estimates trustworthy – especially because, for example, $(2\pi)^3 \approx 10^2$? (3) Do these arguments have predictive power? [Answers: (1) The scaling relations are usually trustworthy. (2) No. In several places, the numerical estimates can be wrong by more than an order of magnitude. (3) No. None of these effects were ever derived by such arguments. However, once the correct result is known from painstaking, rigorous, mathematical analysis – which we shall encounter in rest of the book – such arguments can be provided to "explain" the "physical origin". The true value of these arguments lies in acting as useful mnemonics.]
